The E-Brake

Designing an innovative braking system

by

S.J. van den Heuvel & T.B. Huisman

in partial fulfillment of the requirements for the degree of

Bachelor of Science
in Electrical Engineering

at the Delft University of Technology

July 15, 2017

Supervisors:	dr.ir. H. (Henk) Polinder dr. J. (Jianning) Dong ir. R. (Rick) Lenssen
Thesis committee:	dr. ir. H. (Henk) Polinder dr. J. (John) Schmitz dr.ir. I. (Ioan) Lager

This thesis is confidential and cannot be made public.

TU Delft Delft University of Technology

Abstract

This bachelor thesis is written as part of the curriculum for the bachelor Electrical Engineering at the Delft University of Technology. The thesis is part of the course EE3L11 - Bachelor Afstudeer Project and took place from April 2017 until July 2017.

This document describes the development of a system that is able to drive electric drum brakes, the brake control unit (BCU). The BCU is a subsystem of a larger project; a braking system that minimizes the force between a trailer and a car when braking. The ultimate goal is to let the trailer completely brake for itself.

To achieve this, two other subgroups have designed a control algorithm and a force sensor readout circuit that measures the force. The BCU receives a desired braking force from the control algorithm that should be exerted in order to eliminate the force between car and trailer.
This input force covers a certain range, so the BCU should be designed such that the braking force of the brakes can be regulated. For this purpose a power supply, current controller and lookup table are designed.

The developed power supply is able to provide a constant voltage to the solenoids inside the electric brakes. The power supply consists of a DC/DC converter, which is powered from a car battery. As a consequence, the input voltage of the DC/DC converter is dependent on the state of charge of the battery. Nevertheless, the output of the designed converter is able to provide a constant DC voltage with a maximum current of 8 A.

The designed current controller makes use of a PWM driven current source, which controls the output current of the DC/DC converter. Besides this source, an algorithm that estimates the duty cycle of the PWM signal is derived, based on the desired current through the solenoid.

Last, a lookup table is implemented that determines which current is needed for specific input forces. The table makes use of inter- and extrapolation between measured test results to calculate the right current for every input force.

Contents

1 Introduction

Driving with a trailer has a negative effect on the braking performance of the towing car. Current trailers only make use of an overrun brake, which brakes when the trailer pushes onto the car. The system works with a spring that is located in the hitch connection of the trailer. The spring gets compressed when the car brakes, since the trailer wants to maintain its speed. When the spring gets compressed, a mechanical arm activates the drum brakes. The arm is connected to the braking shoe of the drum brake and when a force is exerted on the arm, the shoes are pushed to the outer shell of the drum brake. The force of braking is dependent on the force between the trailer and car.

Although the trailer is able to brake, the total braking force is not enough to stop the trailer by itself. The trailer still has to make use of the brakes of the car, which are loaded with the extra weight of the trailer.
Another downside of the overrun brake is that there is also a force between the car and trailer when driving downhill. The brakes of the trailer will constantly be activated, resulting in overheating of the brakes.

To counter this problem, the E-Brake project is devised. It is an innovation from the company E-Trailer, a start-up located at Yes!Delft. E-Trailer's vision is to modernize the complete trailer market by combining existing systems with innovative soft- and hardware. The goal of the complete E-Brake project is to eliminate the side effects that driving with a trailer has on braking performance. This can be achieved by designing a braking system that ideally decelerates as much as the car does during braking. By doing so, the car driver experiences no difference in the stopping distance, since the trailer will completely brake for itself.
Furthermore, the E-Brake will detect the angle at which the trailer drives. As a consequence, the system can determine if the brakes should be activated. When the car is not braking when driving downhill, the overheating problem is solved. The project has to be designed around already available electric brakes and a microcontroller board.

Currently, there are no existing systems on the market that use electric brakes to fully brake the trailer on itself. However, there are systems that make use of the existing parking brakes of trailers to contribute to the stopping power. Much trailers have a parking brake installed, which can be activated by pulling a handle at the hitch connection. This handle is connected to two steel cables that run to the drum brakes. When the handle gets pulled, the cables will pull on the parking brake inside the drum brakes. Those systems need to install a powerful servo to the existing brake cables, that sets tension on the cables and thereby make the trailer brake. The downside of these systems is that a servo should be selected that is capable of delivering enough force to pull the cables. Furthermore, it should be accurate enough to be able to regulate the braking force such that the driver in the car feels no influence of the trailer on the braking action. An advantage though, is that these systems are widely applicable for almost every trailer and require very limited adjustments to the trailer itself.

The other option is a system that uses electric brakes. A drum brake gets activated by a solenoid inside the brake, which is a proven concept. Such brakes are already in use in Australia and the United States [21], where the brakes were proven to be reliable. When a current flows through the solenoid, the brake is activated, which will be explained in further detail in section 5.2. A downside of the electric braking system is that it can brake relatively rough. The powering line of the brakes might experience interference of other power lines that run through the trailer [16].

To control the electric drum brakes, various controllers are available. These controllers all contain some sort of accelerometer and use this to proportionally adjust the current that flows through the solenoids [14]. The controllers should be connected to the battery of the car, wires should be installed and connected to the brakes in the trailer. Thus, a downside is that aftermarket installment is a complicated task.

Instead of installing an existing controller, the microcontroller board of E-Trailer is used, the E-Connect. The advantage of using this board is that it can communicate with already existing products of E-Trailer. The braking system can be connected to several sensors that are installed on the E-Connect. Examples are a gyroscope and accelerometer, to determine whether the trailer is driving on a slope. In this situation the brakes should not always be activated, even though there is a force measured between the car and the trailer. This is done by a force sensor in the hitch connection.

Furthermore, an anti-swaying process will be developed in the future as an upgrade on the E-Brake system. To correct the swaying movement of the trailer, present systems simply pull the brakes of the trailer. Instead of slowing down the car-trailer combination, another option would be to brake the wheels of the trailer separately.

Especially for this latter reason, a completely new brake controller should be designed. There are no systems on the market that implement both anti-swaying technology and brake controlling. Since the former technology requires the brakes to be individually driven, the E-Brake system has to be completely designed by itself and cannot make use of existing products, except for the electric brakes.

In order to achieve this, three main sub-projects can be distinguished. The subgroups are depicted in Figure 1.1 and are discussed individually.

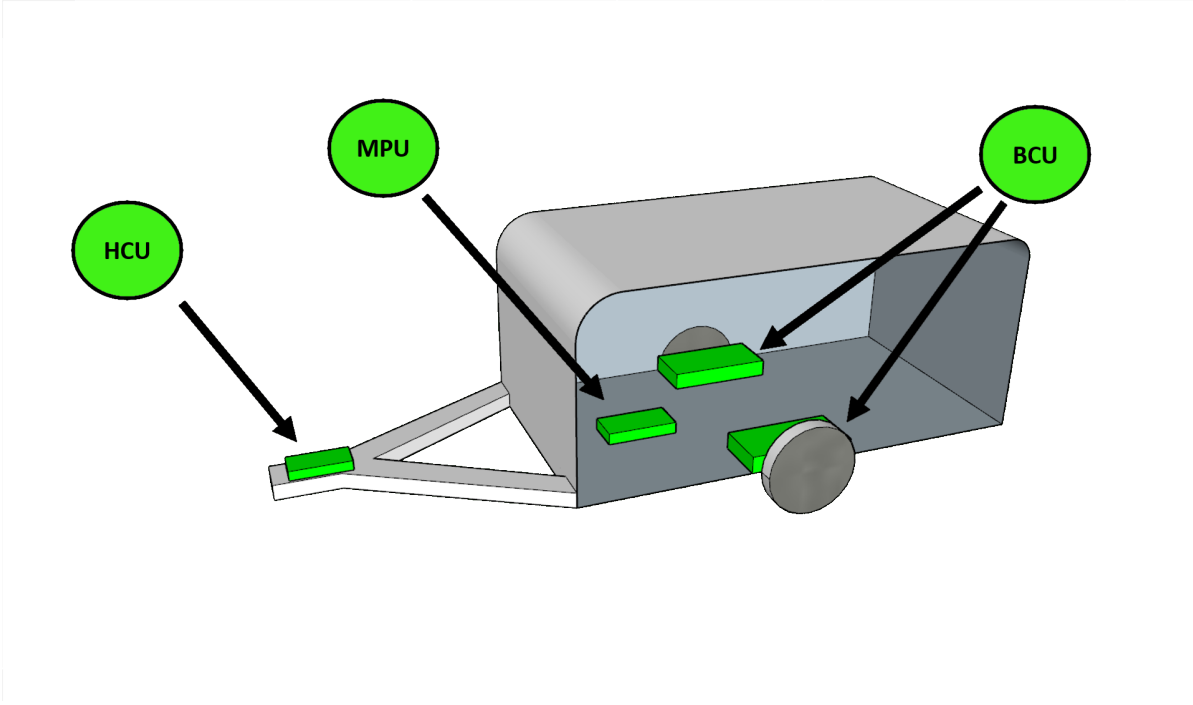

Figure 1.1: An overview of the subsystems in the trailer.

First, there is a force sensor located inside the front of the hitch connection of the trailer. This force sensor measures the force between the car and the trailer. The force should be read from the force sensor, processed and sent to the processing unit, the E-Connect. The part that reads the force sensor is called the hitch connection unit (HCU) and is also responsible to act as a gateway between the systems in the car and the systems inside the trailer. This is done via a CAN-bus, which is the standard bus used in vehicles to communicate between systems.
Second, the force sensor data should be processed to determine whether the trailer should brake. If so, the

appropriate force needs to be calculated. For this purpose the E-Connect is used, which will form the core of the total E-Brake. This main processing unit (MPU) should implement a control algorithm to calculate the braking force. Ideally the measured force on the force sensor whilst braking should go to zero. When there is no force between the car and the trailer, the trailer brakes completely for itself, without the need to rely upon the brakes of the car.
Last, the brakes inside the trailer should be driven in order to achieve the desired braking force. The desired braking force is received from the MPU. Then the brakes should be controlled in such a way that this desired braking force is achieved. This will be the task of the brake control unit (BCU). The system should be designed with the use of already available electric drum brakes. This thesis will describe the design process to implement the BCU, which can, repeatedly, achieve the correct braking force by making use of the electric drum brakes. The remaining subsystems are described by the theses of the other teammembers of the BAP-group.

The total system to be designed should have several components in order to work properly. First the brakes should be powered by a power source. It is enforced by the Dutch law to power the system via a combination of electricity from the car and an extra battery [1]. This battery is located inside the trailer itself, which acts as a buffer when high currents are needed. The design of the power supply is treated in chapter 3.
Second, the current should be controlled by hardware. It should be adjustable and able to quickly respond to changes. The development of such a circuit will be discussed in chapter 4.
Last, chapter 5 describes the mapping of the output current to braking force. The more accurately this can be done, the better and faster the working of the total brake control unit will be.

2

Program of Requirements

This chapter will discuss the program of requirements. In the following sections the functional, ecological and the system requirements are listed. Subsequently any other applicable requirements will be briefly discussed. All the design choices in this bachelor thesis are based on these requirements, as well as the discussion of the performance of the prototype.

2.1. Introduction

As indicated before, this thesis will describe the design and implementation of the BCU. This system is designed based on several requirements, which will be discussed in Sections 2.2 to 2.4. The requirements have been imposed by the RDW[1] or by E-Trailer. The RDW has enforced laws and requirements concerning trailers and their braking systems [1], which are studied extensively to make sure that the E-Brake can be legally used. Since the BCU design mainly focuses on the implementation of the control of the available drum brake, basic requirements applicable to the drum brake itself will be left out of this chapter. Specifications such as “The wheels of the trailer should be able to move without friction when no braking occurs" are already taken into account when the drum brakes were designed by the manufacturer and are not of interest for this project.

2.2. Functional requirements

The functional requirements describe the purpose of the braking system with respect to the total E-Brake. The prescriptions of operation can be found below [1]:

1. The braking system should be able to bring the trailer to a stop.
2. The braking system should be able to regulate the braking action.
3. The braking forces should be distributed equally across the wheels of an axle, unless a safety system, such as anti-lock or anti-swing demands different.
4. The electrical brakes should brake if, and only if a braking signal is received from the MPU.
5. The maximum braking force has to be such that the trailer experiences a deceleration of at least 5.9 m/s^2.
6. The braking system should meet all requirements for all trailer masses equal to or below 1800 kg.

2.3. Ecological requirements

For the ecological requirements the most important aspect to consider is safety. All these requirements are imposed by the RDW and can be found below [1]:

[1] RDW is the Dutch vehicle authority, which controls and creates the legislation concerning the road mobility.

1. The trailer should not swing or move to one side due to braking.
2. The braking system should be reliable in the sense that it will work properly when a braking signal is received, and it will not brake when no signal is received.
3. If a single temporary failure occurs (<40 ms) there should be no distinguishable effect on the braking performance.

2.4. System requirements

The system requirements describe the production, testing and maintenance prescriptions. These prescriptions are mostly determined by E-Trailer and are based on market research and standards in the field. The requirements are [1]:

1. The E-Brake should be made such that aftermarket installation is possible on as much trailers as possible.
2. The solenoid inside the drum brake should not show extensive wear due to overheating.
3. The effectiveness of the braking system should not be influenced by magnetic and/or electrical fields.
4. The electrical braking system should consist of a control device (MPU), an electromechanical transmission device (solenoid) and friction brakes.
5. The electrical control device regulating the voltage for the trailer should be situated on the trailer.
6. The nominal voltage rating should be 12 V.
7. The nominal maximum current consumption shall not exceed 15 A.
8. The relay for actuating the braking current should be situated on the trailer.
9. The response of the braking system should be a maximum of 0.6 seconds in case of an emergency brake.

2.5. Other requirements

In this section the general requirements for the braking system will be listed. All the requirements below are not of interest for this project. However, they are of great importance for the further development of the brake controller [1].

1. The brakes and electrical circuit attached should be weatherproof, e.g. waterproof and mudproof.
2. The power supply of the E-Brake should be sufficient such that when the car engine is running, the brake uses its maximum current and when every electrical device is activated the voltage in the lines will not drop below 9.6 V.
3. The actuation of the braking system via the braking light signals is only allowed when the braking system is connected in parallel with these signal lines.
4. The electrical energy required for the electrical braking system should be supplied by the towing vehicle.
5. A possible (charging) connection between the car's power supply unit and the trailer's battery should be disconnected when braking is applied.
6. If the electrical control transmission fails, the available braking performance should be at least 30% of the total braking force.
7. The testing of the brakes should be executed without locking of the wheels and/or a deviation of the course of the vehicle.

3

Power Supply

In this chapter all the decisions will be described that are made during the design of the power supply for the drum brakes. First, a system overview is given, followed by the basic requirements for the supply. The physical system is divided into two main parts: The power supply, consisting of a DC/DC converter, and a current control module. Design choices of the DC/DC converter will be discussed in this chapter and the next chapter will continue on the current control module.

3.1. Introduction

The goal of the power supply is to provide sufficient power to the current control module in order to drive the solenoid inside the drum brakes. The braking force that is applied to the trailer depends on the force by which the solenoid is attracted to the drum brakes. This force increases as the current increases. For this reason a controlled current source is needed [13], which is in accordance with functional requirement 2. The determination of the maximum required current that runs through the solenoid is based on the Program of Requirements and on practical tests on the drum brakes, which were performed by E-Trailer.

The most important requirements that determine the maximum current are the requirements that indicate the specifications when the system operates at its limits. These are:

- The maximum braking force has to be such that the trailer experiences a deceleration of at least 5.9 m/s^2.
- The braking system should meet all requirements for all trailer masses equal to or below 1800 kg.
- The nominal maximum current consumption shall not exceed 15 A.

To calculate the desired maximum braking force, the required force is calculated for a trailer with a mass of 1800 kg. To be able to decelerate such a trailer, a force of at least ($F = m \cdot a = 1800 \cdot 5.9 =$) 10620 N is needed. In case of a single axle trailer, there are two drum brakes installed, thus each drum brake has to deliver half of the total braking force. In case of multiple axles trailers, the braking force is divided over more brakes which is beneficial. For this reason single axle trailers are considered in this calculation.
After E-Trailer performed some practical tests with a single axle trailer, the conclusion was drawn that the currently used brakes are not able to deliver a braking force this large. The tests show that the two brakes are able to generate a maximum of 6500 N, as depicted in Figure 3.1.

Therefore, functional requirement 6 cannot be met using the available brakes. Still, the brakes are able to stop a single axle trailer that is rated for a maximum of 750 kg. Such trailers are one of the most common single axle trailers, thus functional requirement 6 is altered to a maximum of 750 kg.
For a mass of 750 kg a braking force of at least ($750 \cdot 5.9 =$) 4425 N is needed. From Figure 3.1 can be concluded that a current of at least 6 A per drum brake suffices. This is in line with system requirement 7.

All of this current will flow through the solenoid inside the brakes. Since the solenoids are non-ideal, there is an internal resistance present. This resistance is measured under DC conditions, as the solenoid will mainly

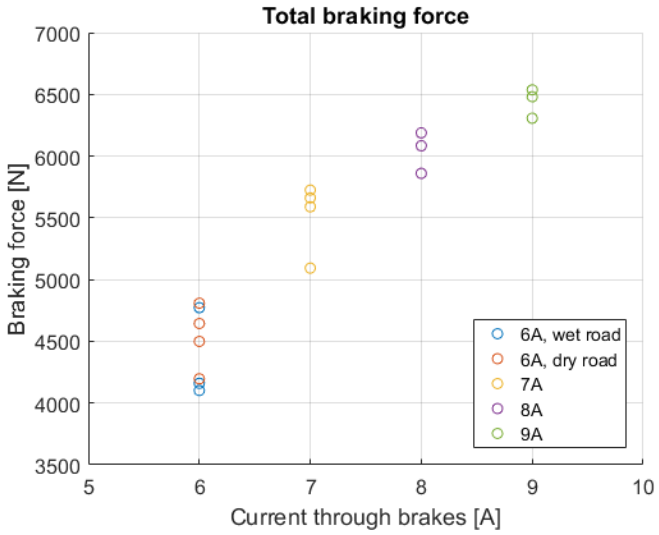

Figure 3.1: The braking force of two drum brakes installed on a single axle trailer.

perform in a steady state. At room temperature the internal resistance of the solenoid is 3 Ω. When the temperature of the coil increases, the resistance will also increase [8]. The solenoid that is used in the drum brake is surrounded by a metal casing that causes the friction and is designed to wear during braking. Therefore only the temperature outside the solenoid can be measured. The result is shown in Figure 3.2.

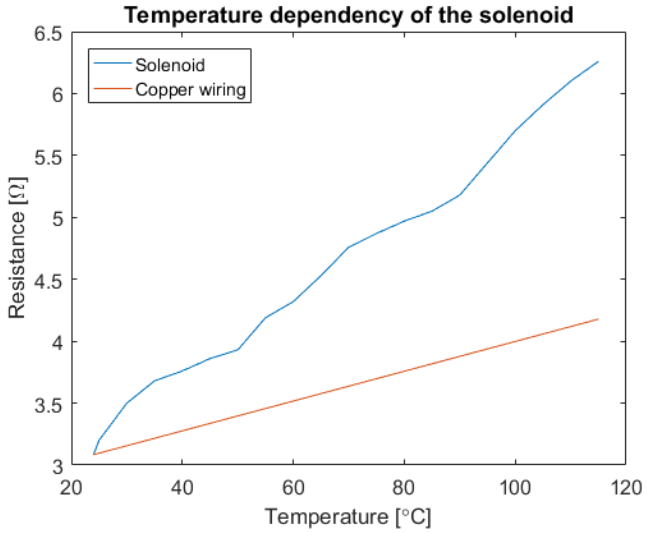

Figure 3.2: The resistance of the solenoid as a function of surface temperature.

In the graph the temperature dependency of copper wire is also plotted. The formula for this dependency is:

$$R = R_0[1 + \alpha(T - T_0)] \quad [20] \tag{3.1}$$

where R is the total resistance, R_0 is the resistance of the material at T_0 °C, α is the temperature coefficient of resistivity of copper, T is the measured temperature and T_0 is the temperature of the known resistance value R_0. As can be seen the resistance of the solenoid increases much quicker with temperature than expected from this formula. This can be explained by the convection model, which will be discussed in more detail in subsection 4.3.1.

During the previously mentioned tests performed by E-Trailer, the temperature at the surface of the solenoid

was measured and never rose above 75 °C. At this point the internal resistance of the solenoid is approximately 4.6 Ω. Therefore a voltage of at least $4.6 \cdot 6 = 27.6$ V is needed across the solenoid.
The next section will describe the suitable topology for the converter.

3.2. Topology

To select the topology of the power supply, the requirements for it should be taken into account. The solenoid needs a constant current through it to behave as intended; as an electromechanical actuator. Since a constant current is needed, the complete power supply should act as a current source. The magnitude of its output should be adjustable to fulfill functional requirement 2. In the basis, the current source will be controlled by the microcontroller of the brakes. The power supply that is used is fed by a battery, which has a constant voltage. Therefore, a voltage to current amplifier is needed.
The basic configuration of a simple voltage to current amplifier is shown in Figure 3.3.

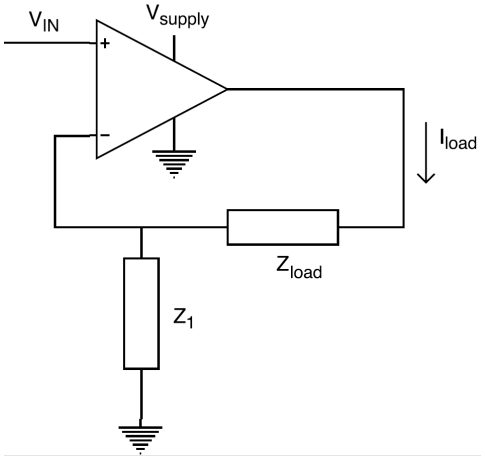

Figure 3.3: A basic voltage to current amplifier topology

The transfer function of this amplifier is:

$$I_{load} = \frac{V_{in}}{Z_1} \tag{3.2}$$

This topology has ideal characteristics in the sense that the input- and output impedance have no influence on the transfer function. However, the configuration is not suitable for high power applications, since operational amplifiers that can create high output currents should be selected. Unfortunately, such amplifiers are very expensive and the circuit will always be limited by the maximum output current of the selected device.

Another topology that can be used is the one depicted in Figure 3.4. The transistor in the circuit is a MOSFET. This is a design choice that will be explained in section 4.2, along with the driving circuit design. A major advantage of this topology is that the output current is only limited by the maximum current of the source, since there are various affordable, high current transistors available. The limited output current makes the topology of Figure 3.3 not suitable for this application and thus the transistor circuit of Figure 3.4 is chosen.

As can be seen in the latter figure the voltage across the solenoid comes directly from the DC source. The supply in a trailer is 12 V coming from a car battery, which is not enough. The 12 V DC voltage should be transformed to a DC voltage of at least 27.6 V. Consequently, a DC/DC converter should be implemented which is able to deliver the 27.6 V and at least 6 A of output current.

3.3. DC/DC Converter

In order to construct the DC/DC converter, the specifications should be considered. Since the supply voltage comes directly from the battery of the trailer, it will not be a constant 12 V. Batteries have an output voltage

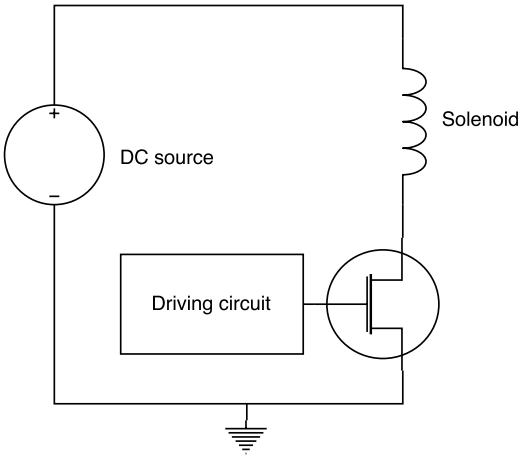

Figure 3.4: The transistor topology.

depending on their state of charge. The voltage will typically fluctuate between 11 and 13 V. As a consequence, the current through the solenoid will fluctuate by $I = \frac{V}{R_{int}}$, with R_{int} being the internal resistance of the solenoid. R_{int} is in the order of several ohms, as indicated in section 3.1. Thus, the current will fluctuate significantly. The variation in current should be minimized, since it also introduces a deviation in braking force. Hence, a constant supply voltage is necessary. This supply voltage should reach higher than the previously mentioned 27.6 V.

Now that the requirements are specified, the topology of the converter has to be chosen. There are various DC/DC converters designed, which all have specific characteristics. Because the output voltage should be higher than the input voltage, the boost topology suits the best [5] [9]. For a boost converter, the standard topology looks as depicted in Figure 3.5.

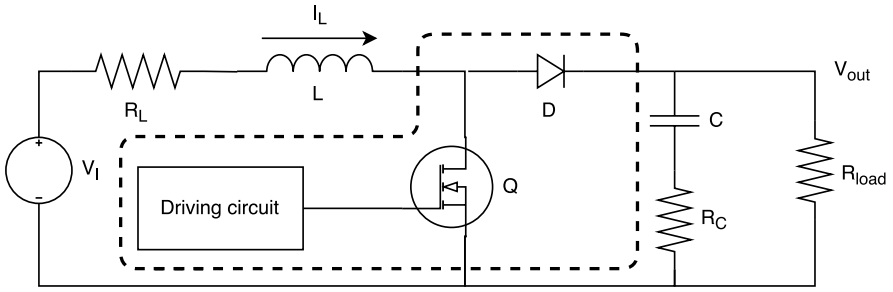

Figure 3.5: A standard boost converter topology.

Q is the switch that causes the inductor current to increase and decrease. When the switch is closed, the current from V_I flows through R_L to L and through the closed switch back to V_I. This is the ON-state of the boost converter. During the ON-state, no current from the source V_I will flow to the output of the converter. However, the current through the inductor will increase with time. Consequently, the voltage drop across the physical inductor (R_L and L together) will increase, because of its internal resistance R_L.
When the switch opens, the OFF-state is introduced and the current will flow from the coil to the diode and into capacitance C and output R. Now the voltage at the output terminal is equal to

$$V_o = V_I - I_L \cdot R_L - V_D \tag{3.3}$$

Because the capacitance tries to maintain a constant voltage across its terminals it stores the energy in the form of an electric field. This means that during the ON-state all the energy that goes to the output is delivered by capacitance C, which reduces its electric field to maintain the voltage over R_{load}.

The complete design of a boost converter is a rather involved task. Besides the circuit depicted in Figure 3.5, the drive circuit should be designed as well, which determines the duty cycle of the PWM signal on the MOSFET Q.
Also, the output feedback should be considered. This measures the output voltage and gives back information to the drive circuit to adjust the duty cycle accordingly. Furthermore, the desired DC/DC converter is a standard boost converter, which means that there are very accurately controlled boost converter chips available on the market. For these reasons the circuit inside the dashed box of Figure 3.5 is bought in the form of an existing boost converter chip. The main advantages of this off-the-shelf chip is that it saves complicated design, it is thoroughly tested by the manufacturer and it is a cheap alternative for the self-designed control circuit.

The DC/DC controller itself is selected on some criteria. First, the chip should be able to output the desired current. Second, the converter should be able to deliver a steady 28 V output voltage for an input voltage swing of 11 V to 13 V. Third, the chip must have a low quiescent current, since it will be connected to a battery inside the trailer. When the trailer is not used for a long period, the quiescent current should not discharge the battery. Last, the chip should be affordable enough to implement it in the E-Brake product.

These search criteria have lead to the LTC3787 of Linear Technology. This chip has a very low quiescent and stand-by current of 135 µA and 8 µA respectively. Furthermore, it is designed as a 2-phase boost converter controller. This means that two boost converter topologies, as depicted in Figure 3.5, are connected in parallel to each other, thereby increasing the output current capacity. These two boost converter channels are 180° out of phase and have the same duty cycle. This decreases the output capacitor ripple current. Consequently, the output capacitance of the total boost converter can be relatively low compared to two single, in-phase boost converters.

The desired DC/DC converter should be able to deliver 6 A at 28 V, as stated before. The circuit displayed in Figure 3.6 meets these requirements and is chosen. This is one of the typical applications of the LTC3787.

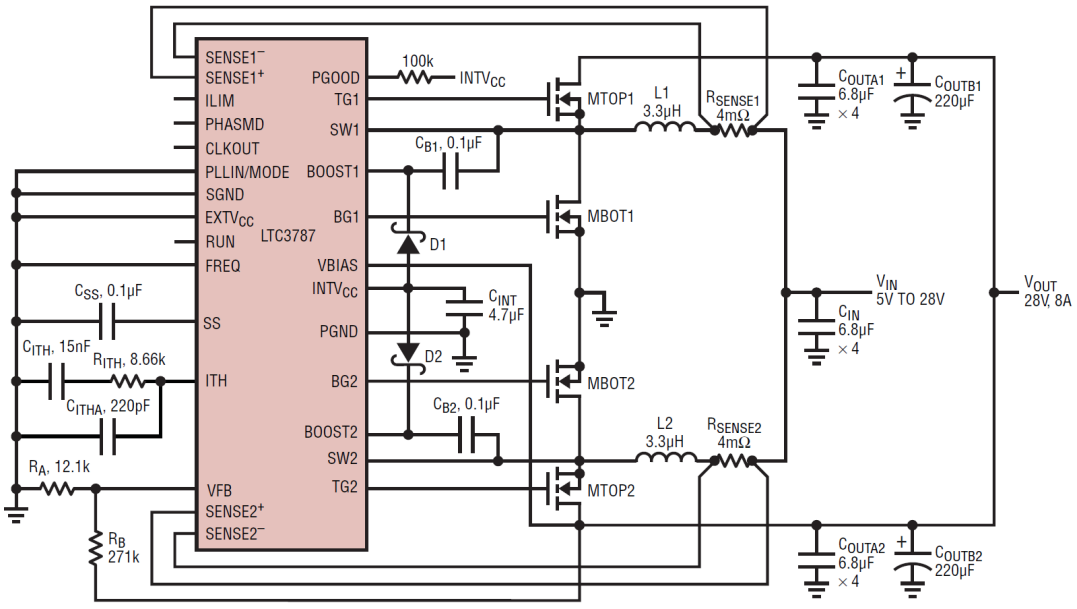

Figure 3.6: The 2-phase synchronous boost converter topology [19].

In the figure the 2-phase synchronous converter is clearly visible. One can see that multiple in- and output capacitors are used in parallel. This lowers the equivalent series resistance (ESR) of the total output capacitance. Ideally the ESR of a capacitor should be as low as possible to prevent any voltage ripple to occur. Therefore, multiple low ESR capacitors are chosen in parallel to minimize the output voltage ripple, which is given by:

$$\Delta V = I_{L(max)} \cdot R_{ESR} \tag{3.4}$$

One of the design considerations is the switching frequency selection, which is a trade-off between component size (and thus costs) and efficiency. The lower the switching frequency, the higher the efficiency of the DC/DC converter. However, the output capacitors and the inductor should be larger in order to maintain a low output ripple. When the frequency increases, the efficiency will drop, although smaller components can be used [19].

Another design trade-off is the way the current is sensed. Either a current sensing resistor can be used, as implemented in Figure 3.6, or DCR sensing can be used. DCR sensing measures the voltage drop across the internal DC resistance (DCR) of the inductor. The advantage is that it does not require a sensing resistor and as a consequence it will be more efficient. The DCR sensing circuit is shown in Figure 3.7.

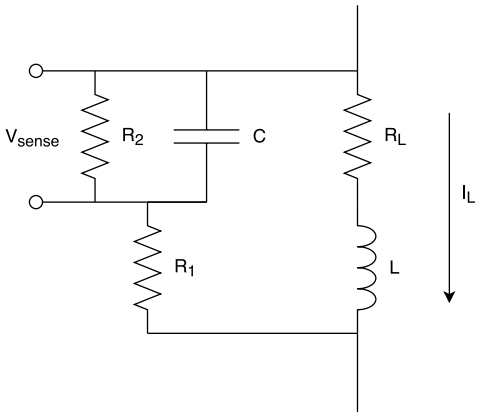

Figure 3.7: The DCR sensing circuit.

This circuit replaces the R_{sense} resistor in Figure 3.6. The accuracy of this way of measuring is, however, much lower compared to the current sensing technique with a sensing resistance. For the E-Brake application, the output current should be as accurate as possible since it determines the braking force. A deviation in braking force is undesired and should be avoided as much as possible. For that reason the current sense resistor is used.

For the value of the inductor, the trade-off between switching frequency and component size should be considered, as well as the resulting ripple-current. The higher the inductor value will be, the lower the ripple-current. The relationship between the inductor ripple-current, switching frequency and inductor value is calculated below.

The duty cycle is defined as

$$D = 1 - \frac{V_{in}}{V_{out}} \tag{3.5}$$

To determine the inductor ripple current ΔI_L the ON-state is considered, where only the voltage source and the inductor are connected. The current ripple then is:

$$V_{in} = L \cdot \frac{dI_L}{dt} \tag{3.6}$$

$$\Delta I_L = \frac{V_{in} \cdot \Delta t}{L} = \frac{V_{in}}{f_s \cdot L} \cdot D \tag{3.7}$$

$$\Delta I_L = \frac{V_{in}}{f_s \cdot L} \left(1 - \frac{V_{in}}{V_{out}}\right) \tag{3.8}$$

To determine the inductor value, a good estimation for the inductor ripple current is $0.2 \cdot I_{max}$ to $0.4 \cdot I_{max}$ [6]. For the switching frequency 535 kHz is chosen, as a compromise between efficiency and inductor ripple current. The LTC3787 is able to work on a programmable frequency range of 50 kHz up to 900 kHz. Since

both efficiency and reduction of ripple current are equally important, 535 kHz is a good trade-off. Rewriting Equation 3.8, and filling in the remaining parameters, the inductor value is calculated as:

$$L = \frac{V_{IN}\left(1 - \frac{V_{IN}}{V_{OUT}}\right)}{\Delta I_L \cdot f_s} \approx 4\,\mu H \tag{3.9}$$

Figure 3.6 shows the opted circuit topology for the boost converter by Linear Technology. The implemented DC/DC converter makes use of the calculated inductor value above, instead of the 3.3 µH inductor.

The MOSFETS used in the boost converter are selected based on the gate threshold voltage, current rating, voltage rating, switching frequency and on-resistance. The LTC3787 has gate driving pins with 5.4 V outputs, thus logic level MOSFETS should be purchased in order to work properly. Furthermore, the maximum voltage rating should be high enough in order to use it in the circuit, typically 50 V rated MOSFETS are used. These transistors should have a switching frequency of at least 535 kHz in order to perform as wanted. The last criterion is the resistance when completely switched on, or $R_{DS(ON)}$. The lower the on-resistance will be, the less power is dissipated inside the transistor when conducting.

The input and output capacitors should be large enough to keep the input and output voltage ripple as low as possible. A low output voltage ripple also includes a low internal resistance of the output capacitor, the ESR. The ripple, due to the ESR, is given as $\Delta V_{ESR} = R_{ESR} \cdot I_{L(max)}$ and thus a low ESR is desired.

4

Driving the Solenoid

4.1. Introduction

The design of the electric controlled brakes is such that the braking cables are replaced by a solenoid. This solenoid clings itself tightly upon the cast iron of the rotating wheel when it is magnetized. This way the arm connected to the solenoid makes the braking shoes expand and brake the trailer. The braking force is determined by the friction force between the braking shoes and the drums, but also by the friction force between the solenoid and the cast iron. The latter friction force is dependent on the magnetic field the solenoid creates and that field is dependent on the current flowing through. Thus, in order to control the solenoid a current module is needed.

Initial requirements, which the current control module should meet are:

1. It should be able to handle and drive a maximum current of 6 A.
2. The current it emits should be predictable and dependent on duty cycle. More precise: The actual current should be within a deviation of 100 mA of the intended current.

The chapter is divided in several subsections. First the control signal is determined along with its consequences. After that, issues on the solenoid are discussed. Then the relationship between the duty cycle and the current is determined. Last, the chapter continues with the actual design and implementation of the module.

4.2. The control signal

This section will describe the design choices that are made concerning the current control module.

There are several options to convert the control signal of the processor used by the HCU. It can be done by either using a linear regulator or by using a switching regulator. Two main considerations are described below.

- The most important disadvantage of the first one is the power loss that is associated with it. When a transistor is used in its active or linear region, its resistance is higher than its resistance in saturation or switching mode.
- The most important disadvantage of the latter one, the switching regulator, is that the switching causes additional noise and ripples at the output.

The power losses outweigh the additional noise and ripples, so a switching regulator has been chosen which implies that a PWM signal is needed as the control signal.[10] [23]

There are basically two different ways to convert the PWM signal in order to control the current flowing through the solenoid. It can be realized either by using a bipolar junction transistor (BJT) or by using a metal-oxide-semiconductor field-effect transistor (MOSFET). A BJT is a current driven device and a MOSFET is a voltage driven device.[18]

Further exploration of the two devices will be done below, first the advantages of a BJT over a MOSFET are listed.[18]

- A BJT has a higher amplification capability than a MOSFET.
- A BJT is less expensive than a MOSFET.

And below the advantages of a MOSFET over a BJT are listed.

- A MOSFET has a higher input impedance, which means lower losses at the gate.
- The amplification factor of a BJT is lower than that of a MOSFET. This means that a BJT handling high currents also needs a high drive current.
- The switching frequency of a MOSFET is higher than that of a BJT.
- The ON-state resistance of a MOSFET is lower than that of a BJT. This means less energy is dissipated when the MOSFET is in its ON-state.

To summarize, the main advantages of a BJT are its high amplification capability and its lower costs.
The main advantages of the MOSFET are the higher switching frequency and the lower losses.
The decisive advantage is the lower energy consumption of the MOSFET over the BJT. However, before selecting this device as the best, another switching device needs to be considered.

Besides these two basic options there also exists a possibility to combine the principle of a MOSFET and BJT, resulting in an insulated gate bipolar transistor (IGBT). The IGBT offers the best of both devices in one device. The device can be explained as follows:
It uses the MOSFET as an input stage (the driving circuit) and the BJT (the main circuit) as the output stage. Although there are big advantages, like being capable of handling higher power flows and fast switching frequencies, it is questionable whether these specifications are needed or not. Therefore, a look has been taken at the disadvantages. Obviously the costs of this device are higher than that of a BJT or a MOSFET. Moreover, there is an increase in voltage drop over the emitter and collector of the IGBT compared to the MOSFET.[18] Since there is not much tolerance with the current topology and the typical voltage drop is twice the voltage drop across a MOSFET or BJT for an IGBT, these losses are simply undesirable. Consequently, the MOSFET remains the chosen device for the switching transistor. The advantages of an IGBT do not outweigh its disadvantages.

4.3. Non-idealities of a solenoid

A solenoid in itself is a long, (often) copper wire, which is wound close to each other. One can imagine that a long wire introduces a certain resistance and therefore in practice a coil is modelled as an ideal coil and a resistor in series. [17] This model is a better representation of reality, but it still has imperfections. Below the most common complications are discussed.

4.3.1. Temperature effects

Because of the internal resistance of the solenoid, the temperature increases due to dissipation. The internal resistance increases as well as a consequence of the rising temperature. Another heat source is the friction of the coil upon the cast iron. This friction causes the brakes to be able to actually brake. The relation between the temperature of the coil and the resistance of it is depicted in Equation 4.1. [8]:

$$R = R_0[1 + \alpha(T - T_0)] \quad [20] \tag{4.1}$$

As already discussed in section 3.1 the temperature measurements do not agree with the expected value's that Equation 4.1 predicts. This is due to the fact that the measurement point is not directly on the copper of the coil but outside its casing. Convection takes place at the outsides of the solenoid. Besides, there is an extra heat source, namely the heat caused by the friction between the cast iron and the solenoid during braking. A one dimensional electric analog of the situation where heat generation is assumed uniform is displayed in Figure 4.1

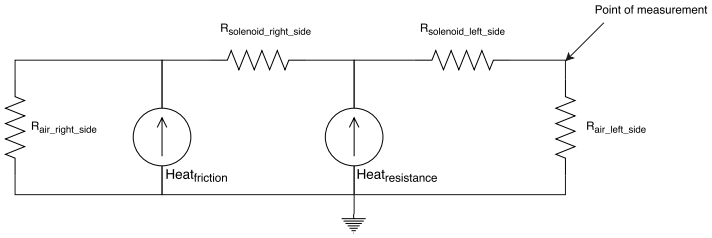

Figure 4.1: An electric analog of the heat convection

During measurements the heat source due to friction was zero. Therefore, a linear dependency between the measured resistance values and the expected ones is observed. [11]

4.3.2. Skin effect

Another non-ideality of coils, is that they show skin effect. AC currents induce an associated magnetic field. This alternating magnetic field in his turn induces a current. At the boundaries of the wires this induced current has the same direction as the original current. However, at the center it opposes this direction. As a result, the AC current tends to flow at the boundaries of a wire instead of flowing uniformly. Consequently, the resistance of the wires increases as the frequency increases. Figure 4.2 illustrates what happens inside the wires and Equation 4.2 describes the mathematical relation between frequency and resistance. [8]

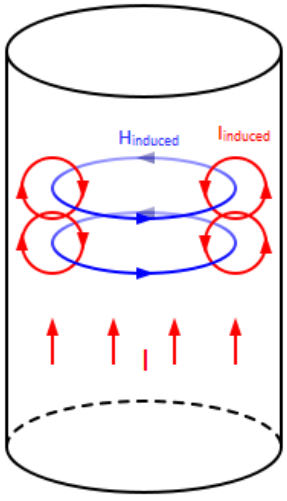

Figure 4.2: An illustration of the skin effect

$$R_{ac} = \frac{R_{dc} \cdot r_{wire} \cdot \sqrt{\pi \cdot f \cdot \mu \cdot \sigma}}{2} \tag{4.2}$$

It is difficult to determine all parameters needed for this relation. Though, since the coil will be driven by PWM, most of the frequency components are just DC and therefore it is assumed that this effect plays no significant role in this application.

4.3.3. Proximity effect

A related effect that can be present is called the proximity effect. Since the wires of the coil are closely adjacent to each other, the induced magnetic field of an AC current influences on the other wires. As a result, Eddy currents are induced in the adjacent wires. The consequence of this is the same as the consequence of the skin effect, namely that the current does not flow uniformly across the surface. That means that due to this effect the resistance increases even more. The resistance that results from this effect is related by Equation 4.3. [8]

$$R = R_{ac} \cdot (1 + k_f(\phi_m - 1)) \tag{4.3}$$

As can be seen the resistance depends on R_{ac}, k_f and on ϕ_m. k_f is a function which is zero for very low frequencies and ϕ_m is the ratio between the coil resistance and a straight wire resistance for high frequencies. For DC this ratio is just one.
The same story as for the skin effect holds here, since mainly DC components are present in the current flowing through the coil the resistance due to the proximity effect is neglectable.

4.3.4. Saturation

The magnetic field of coils tends to saturate due to saturation of the core at a certain point. This is expected to take place with the solenoids inside the drum brakes as well. Since no datasheet nor specifications are available of the solenoids the influence of saturation will have to be checked when testing the system. Tests performed by E-trailer show no significant influence using currents up to 6 A. Therefore for this system probable saturation is not taken into account. [4]

4.4. Model analysis

In section 4.2 there has been explained why a PWM driving circuit is being used. The main reason for this was that there is less power loss. By using PWM the voltage across the coil will switch from zero to more or less the output voltage of the DC/DC converter. The relation between the current and the voltage of a non ideal coil is stated by Equation 4.4:

$$V = L \cdot \frac{dI}{dt} + I \cdot R \tag{4.4}$$

As the $\frac{dI}{dt}$ indicates: The current in the coil does not change instantly. Although the current path is being blocked by the MOSFET as it turns off. The coil opposes this sudden change in current and induces a current with associated voltage. The coil sees an infinitely high resistance but wants to retain its current. Dictated by Ohm's law, huge voltage spikes are introduced. To prevent this from happening, a diode is placed parallel to the coil where the current can easily pass if the path to ground is disconnected. The current loops through the coil and the diode as the energy is being dissipated by the non-ideal effects of the coil and the diode.

The topology of the current driving module is displayed in Figure 4.3

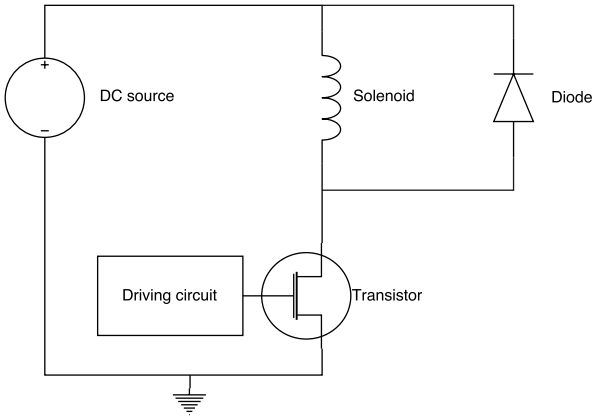

Figure 4.3: The topology of the current driving module

If the coil is split up in a resistance and an ideal coil, then for the ON and OFF states of the MOSFET the following circuits are relevant: (Figure 4.4)

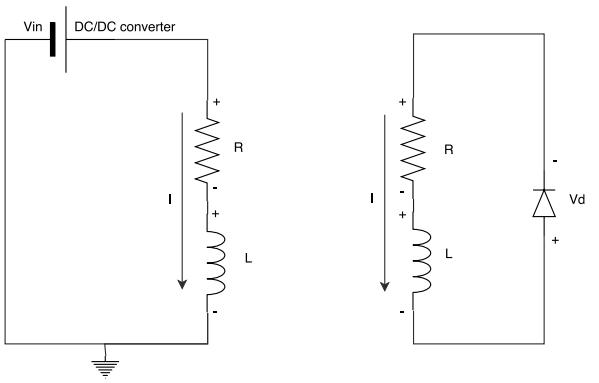

Figure 4.4: The circuits belonging to the ON(left) and OFF(right) state of the MOSFET

In these circuits the resistance of the diode and the resistance of the MOSFET during the ON state are neglected, because they will be small enough to neglect with respect to the resistance of the coil.

Analyzing both circuits by Kirchhoff's voltage law gives:

- ON state (left):

$$\frac{\delta I}{\delta t} \cdot L = V_{in} - R \cdot I \tag{4.5}$$

- OFF state (right):

$$\frac{\delta I}{\delta t} \cdot L = R \cdot I + V_d \tag{4.6}$$

In order to derive a function which determines what duty cycle is needed for which current, these two formulas need to be combined. For this purpose, the time of the ON state is indicated by d and the time of the OFF state is indicated by 1-d, in such a way that one cycle of ON and OFF takes the time unit of 1.

The coil will mainly operate in stabilized mode so that the voltage drop across the coil during the discharging time (1-d) is the same as the voltage increase during the charging time (d). Therefore, the analysis of the circuit and its transfer function should be valid for this stabilized mode. This simplifies the analysis because known is that:

$$\Delta V_{L_{ON}} = \Delta V_{L_{OFF}} \tag{4.7}$$

and

$$V_L = \frac{\delta I}{\delta t} \cdot L \tag{4.8}$$

Combining Equation 4.5, Equation 4.6, Equation 4.7 and Equation 4.8 gives:

$$\int_0^d V_{L_{ON}} \delta t = \int_d^1 V_{L_{OFF}} \delta t \tag{4.9}$$

$$(V_{in} - R \cdot I) \cdot \int_0^d \delta t = (R \cdot I + V_d) \cdot \int_d^1 \delta t \tag{4.10}$$

$$(V_{in} - R \cdot I) \cdot d = (R \cdot I + V_d) \cdot (1 - d) \tag{4.11}$$

$$(V_{in} + V_d) \cdot d = R \cdot I + V_d \tag{4.12}$$

$$d = \frac{R \cdot I + V_d}{V_{in} + V_d} \tag{4.13}$$

Transient analysis is not needed for this application because the input variables of the model are updated at a maximum speed of 200Hz by the processing module of the HCU. This means that there is T = 1/f = 1/200 = 50 ms of time to stabilize. The time constant τ of the RL system that is used is L/R, which corresponds to about 2.7 ms. In the worst case scenario the coil needs to be fully charged and in the next cycle needs to be discharged. This situation is not likely to occur, since the MPU module will be sending abrupt braking changes in several cycles or else the driver will experience discomfort from the braking trailer.

4.5. Implementation

To actually drive the solenoid the circuit design has to be made and the circuit should meet its requirements. This section discusses this subject. It starts with deriving the decision of the switching frequency. Then it continues with the design of the circuit and its components.

4.5.1. The switching frequency

The basic driving circuit for the solenoid yet consists of a MOSFET and a diode. In order to define all important component specifications for the circuit parts, first the switching frequency of the PWM signal needs to be determined. Relevant issues for this decision are:

- The current ripple needs to be acceptable.
- The switching time losses.
- The system components, for example the processor, need to be capable of handling the frequency.

The first item indicates a lower boundary for the selection of the switching frequency. The latter two limit the switching frequency with an upper boundary. The maximum current ripple that is acceptable is 50 mA. This current change is established empirically and is not perceptible in the car. There has been taken some margin here, up to 100 mA is still hardly perceptible.

Starting with Equation 4.5 and Equation 4.6, the frequency that specifies the lower boundary is derived as follows:

$$\frac{\Delta I_{ripple}}{\Delta t_{on}} = \frac{V_{in} - R \cdot I}{L} \tag{4.14}$$

$$\frac{\Delta I_{ripple}}{\Delta t_{off}} = \frac{R \cdot I + V_d}{L} \tag{4.15}$$

The total time of one cycle is then:

$$t_{total} = \Delta t_{on} + \Delta t_{off} = \frac{\Delta I_{ripple} \cdot L}{V_{in} - R \cdot I} + \frac{\Delta I_{ripple} \cdot L}{R \cdot I + V_d} \tag{4.16}$$

The total switching time is dependent on the current. All current values between 0.6 and 6 A are within the possible range and should not exceed the maximum ripple. The derivative is taken to find out what the maximum frequency is that defines the lower boundary.

$$\frac{\delta t_{total}}{\delta I} = \Delta I_{ripple} \cdot L \cdot (\frac{R}{(V_{in} - R \cdot I)^2} - \frac{R}{(R \cdot I + V_d)^2}) = 0 \tag{4.17}$$

For calculating what current defines the maximal frequency the input values that are used are:
$V_{in} = 28V, V_d = 0.6V, R = 3\Omega, L = 8mH$ and $\Delta I_{ripple} = 50mA$

$$I = \frac{V_{in} - V_d}{2 \cdot R} = 4.57A \tag{4.18}$$

$R = 3\Omega$ is used because this is the resistance for the coil as it is the coldest. An increase in resistance due to heat would be advantageous for the cycle time. Filling in Equation 4.16 with this current gives a frequency of about 18 kHz as a maximum, this is the lower boundary.

The second item not really define a boundary but more or less states that the switching frequency needs to be as low as possible so that the losses that occur during switching are minimal.
For the switching components used in the circuit to drive the solenoid though the switching time will be as low as maximally 1 % of the total cycle time. This requirement is set to limit the losses in the circuit.

The third item has mainly to do with the processor that handles the PWM output. This processor can accurately emit the PWM signal up to 30 kHz so this frequency sets the upper boundary of the switching frequency selection.

A switching frequency of 20 kHz has been chosen because it is possible that not all solenoids will have exactly the same inductance. Taking the switching frequency slightly higher than the lower boundary allows this deviation of inductance so that the solenoids still meet the maximum rated ripple. The other reason for choosing this frequency has to do with the second item, namely that the switching frequency should be as low as possible.

4.5.2. Circuit design

The component selection concerns for the MOSFET and the diode are as follows. Both components need to be able to switch at 20kHz and the time of switching may not exceed 1 %. Also the resistance in conduction mode of both should be as low as possible so that the assumption that they are negligible remains valid. As a requirement for the MOSFET, the R_{DSon} should be less than $8.33m\Omega$. In the extreme case of a current as big as 6 A, this results in a voltage drop of 50 mV over the MOSFET. Then they both have to be able to handle the power that they take and handle. A safety margin of 6 times the rated current should be sufficient in this case.

Since one of the aims of the total current control module is to convert a CPU signal into a rather high current, it has been chosen to use a pair of opto-couplers between the processor and the PWM driven MOSFET. These prevent damage to the processor in case something goes wrong or breaks down in the high current circuit.

The main component selection concerns for this pair of opto-couplers is that they can handle 20 kHz and that the switching time is less than 1 %. Furthermore, it should be possible to drive it with 5 V.

The diode of the opto-couplers needs to be driven by the PWM output of the processor. In order not to load that pin, a transistor will be used with its drain connected to the 5 V supply of the processor and a resistor in series to the diode and the transistor to establish the right current for the diode.
The gate will be driven by the PWM output pin. The main concerns of choosing this transistor is that it can handle the 20 kHz and that its switching time is less than 1%. Also it should be driven by 5 V.

The total circuit design now is as follows:

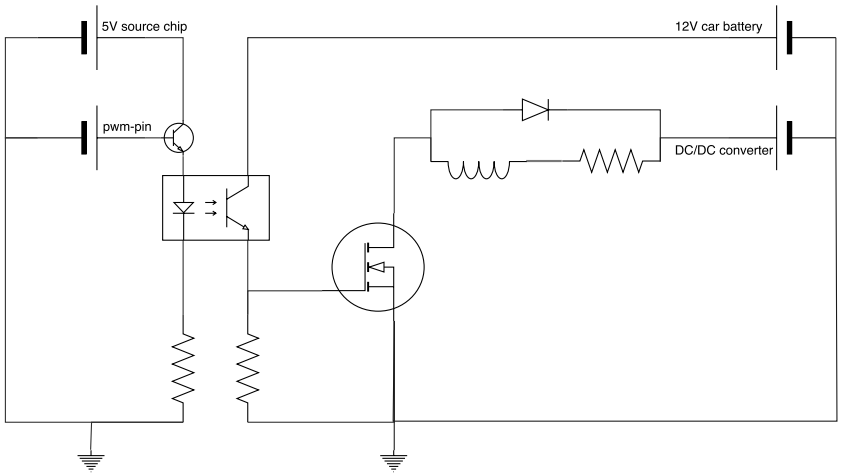

Figure 4.5: The total current control module circuit

As can be seen the small signal circuit is isolated from the high current circuit by light. They do not share the same grounds.

As explained in section 4.3 the resistance of the coil will vary dependent on the temperature of the coil. There is a possibility that the actual current is not consistent with the calculated current. Another possibility is that the battery voltage sags and delivers too little power that the DC/DC converter can not cope with and the voltage across the solenoid is not equal to the ideally expected 28 V. For this issue a PI controller has been designed by the MPU group. In order to make this control loop function properly, the actual current flowing through the solenoid is needed. A current sensor is needed whose readout circuit is also separated with the high current circuit. The current sensor should be able to measure up to 6 A minimum. The updated circuit is displayed in Figure 4.6.

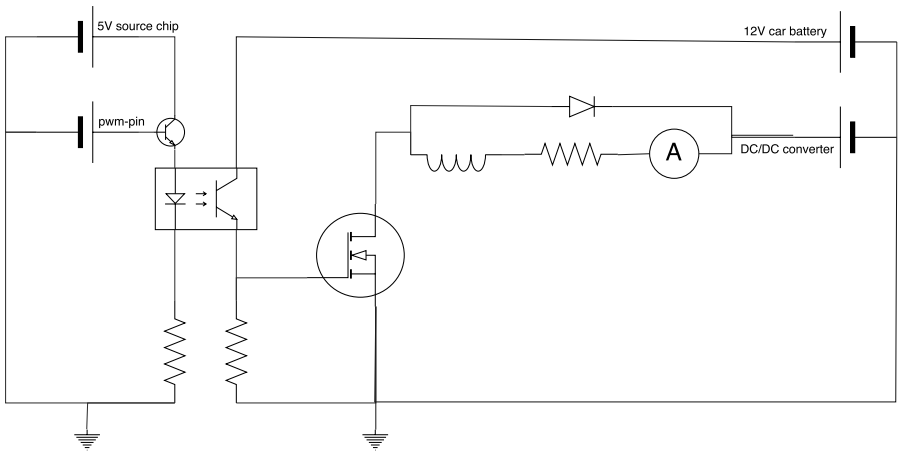

Figure 4.6: The total current control module circuit

5

Lookup Table

In this chapter the design and implementation of the method that maps the exerted braking force to an input current will be described. First, the different options are discussed and weighed against each other in **??**. Then, the best option is chosen and implemented. This is discussed in section 5.3. The chapter ends with results of the implemented method in section 5.4

5.1. Introduction

As mentioned before, the inputs of the brake control unit that come from the other systems in the total E-Brake are the temperature of the brakes and a desired braking force. The braking force is calculated by the measured force of the force sensor and adjusted by the control algorithm of the MPU. The task of the mapping method is to process these inputs and calculate the desired current. This calculated current should be approximately equal to the received current from the MPU. Two methods are chosen and weighed against each other in the next section.

5.2. Mapping methods

One way to map the force and temperature to a current is with the use of a model of the complete drum brake. An overview of the drum brake should be made and certain parameters need to be determined, such as friction coefficients and self-clamping effects. Another approach is the creation of a lookup table (LUT). The basis of a LUT is a large collection of test data, which is processed into a large array. By writing software that inspects the table when certain temperatures and forces are received, a current can be calculated.

5.2.1. Model of the drum brakes

The model of the brake has to take the entire working of the drum brake into consideration. The available drum brake is depicted in Figure 5.1, which is studied extensively.

The drum brakes work according to a lever. The oval solenoid in the bottom of the brake gets magnetized and attracted to a cast iron outer shell. Figure 5.1 only shows the inner side of the drum brakes, which is attached to the trailer. In the bottom the oval solenoid is clearly visible, just as the golden colored lever that pushes the braking shoes apart from each other. In Figure 5.2 a regular drum brake is depicted with the cast iron drum. The brake in Figure 5.1 has the same drum, to which the wheels are mounted.

When current flows through the solenoid, a magnetic field is created. This field attracts it towards the drum, such that a clamping force arises. This clamping causes friction, as the drum rotates with the wheels of the trailer, but the solenoid is limited in its movement. The clamping force of the solenoid to the drum is the normal force in this case, and the resulting force of friction tries to pull the solenoid in the rotational direction of the drum. The solenoid is attached to one side of a lever and the other end is attached to one of the braking

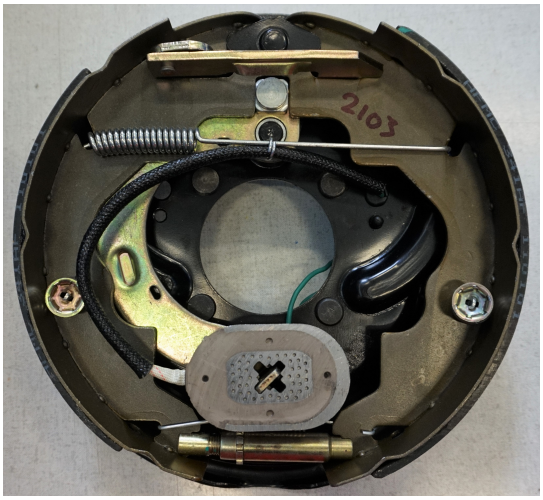

Figure 5.1: The used drum brakes in the E-Brake system.

shoes. Because the solenoid moves along with the drum, the braking shoes are pushed to the drum as well, via the lever. Again a friction force is created, which is the main component in the total braking force. When the current through the solenoid increases, the magnetic field also increments. Consequently, the normal force increases, which raises the frictional force of the solenoid. The frictional force of the braking shoes also increases because of the lever they are attached to. Via this leverage effect the stopping power can be regulated.

From this first observation a number of transfer mechanisms can be distinguished:

1. The transformation of a current into a magnetic field
2. The transformation of the magnetic field in a force of attraction
3. The transfer of the attraction force between the solenoid and the drum to a frictional force
4. The transfer of the frictional force of the solenoid to a normal force on the drum shoes via the lever
5. The transfer of the normal force on the braking shoes to a frictional force

The first transformation makes use of Equation 5.1:

$$B = \mu_0 \cdot \mu_r \cdot n \cdot I \tag{5.1}$$

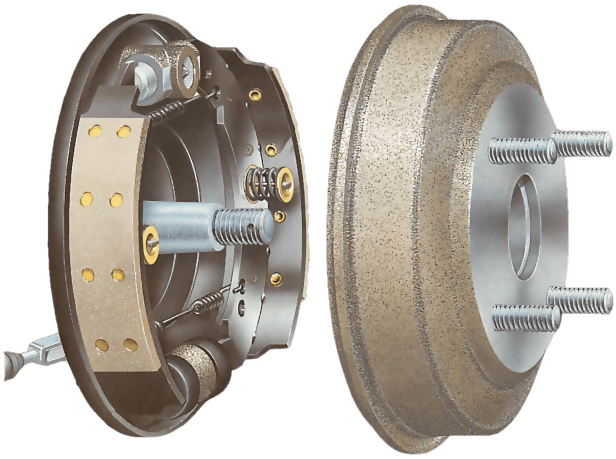

Figure 5.2: The drum and the inner side of a regular hydraulic drum brake [22].

Here B is the magnetic flux density, μ_0 is the permeability of vacuum, μ_r is the relative permeability of the material of the core of the solenoid and n the turn density in turns per meter.

The magnetic flux density then has to be transferred into a force of attraction. The magnitude of the resulting force is dependent on many coil parameters, as can be seen in Equation 5.2 [12].

$$F = \frac{1}{2} i^2 \frac{dL}{dx} = \frac{1}{2} i^2 \frac{N^2 \cdot \mu_0 \cdot A}{\left(g + x_m - x\right)^2} \tag{5.2}$$

Here F is the force provided by the solenoid, i is the current in the winding, N is the number of windings, A is the cross sectional area of the solenoid, g is the bearing thickness, x_m is the maximum travel of arm with zero current and x is the actual travel of arm.
As Equation 5.2 shows, the reluctance force is an involved formula, which depends on many parameters. For the case of the solenoid, the bearing thickness is not applicable, but the other parameters need to be determined.
The force of attraction then is converted into so called dry friction, which means that two solid surfaces act upon each other with no fluids or lubricants involved. The formula for dry friction is given by Equation 5.3.

$$F_f \leq \mu \cdot F_n \tag{5.3}$$

Here F_f is the force of friction, μ is the coefficient of friction, which is material dependent, and F_n is the normal force, in this situation the force of attraction. In the case of dry friction, μ is among others dependent on speed and temperature [3]. Consequently, the rather simple looking Equation 5.3 actually is a complex system, which takes many parameters into account.

For the working of the lever, Equation 5.4 can be used, which relates the force of friction on the solenoid end to the normal force delivered to the braking shoes on the other end of the lever.

$$F_n \cdot x_{shoe} = F_f \cdot x_{solenoid} \quad \rightarrow \quad F_n = \frac{F_f \cdot x_{solenoid}}{x_{shoe}} \tag{5.4}$$

Here $x_{solenoid}$ and x_{shoe} are the distances of the solenoid to the turning point and the braking shoe to the turning point respectively. Again the resulting force of friction at the braking shoes should be determined using Equation 5.3.

There are several problems with the modelling of the complete drum brake. First, the determination of the reluctance force is a rather involved process, since the exact behaviour and characteristics of the solenoid inside the drum brake are unknown. The exact position that the solenoid has to travel is imprecise. Bumps in the road affect the position of the solenoid, which causes inaccuracy in the model.
Also, the material of the core is unknown, and as a consequence, so is the saturation of the core. Furthermore, the force of attraction depends on the position of the solenoid relative to the cast iron drum, as Equation 5.2 shows. The air gap between the two continuously changes with respect to time when a current flows through the solenoid.
As stated before, the coefficient of friction is dependent on several parameters as well. Besides the earlier mentioned rotational speed of the drum and the temperature, there are more dependencies: the material of the outer side of the solenoid, the material of the braking shoes, the state of wear of the shoes, weather conditions and road conditions. When the trailer would drive through a puddle for example, water comes into the brakes, and the dry friction model is suddenly not that accurate anymore. Even the normal force of Equation 5.3 is not uniformly distributed across the braking shoe [7], which makes accurate prediction of the force of friction even more difficult.
The above influences and dependencies affect the accuracy of the model of the brakes. Therefore, another solution is opted, which will be discussed in the next subsection.

5.2.2. Lookup Table

A second option to map the resulting braking force to a current is the creation of a lookup table (LUT) that is based on test results. By performing tests at which constant currents flow through the solenoid and collecting the exerted braking force, the table can be created.
When a braking force and a certain temperature of the brakes are received, a programmed code will search

the table for the appropriate current. The LUT will be implemented in an array. Since not every point of operation can be specified in the array, other points are estimated using linearization between two measured points. In this way the LUT is as accurate as possible, estimating points instead of mapping to the nearest saved value.
Some advantages of the lookup table over the model of the brake are its simplicity and the time of creation. Instead of trying to model the complete non-linear behavior of the drum brake, data is collected which is used as a first estimation of the appropriate current. In the end, the creation of a lookup table may even result in more accurate estimations, since the model has many uncertainties as described above. The physical testing already takes all the effects into account, and therefore this option is chosen.
A drawback of the LUT is that all the data it holds is only very precise at certain conditions; the same conditions as during testing. With the use of inter- and extrapolation a lot of inaccuracy can be removed, but wear and weather conditions are not included in the LUT. For the former problem, the LUT can be made self-adjusting or programmed to save extra data when the calculated current deviates too much from the eventually achieved current determined by the control algorithm of the MPU. This is, unfortunately, out of scope for this thesis, but will be discussed in chapter 9.

5.3. Test data

The gathering of test data is done making use of two different test set-ups. For each of the set-ups the collected data and peculiar results will be discussed.

5.3.1. EWI set-up

The set-up at EWI consists of one single brake, that is attached to an electric motor via an axle, as can be seen in Figure 5.3.

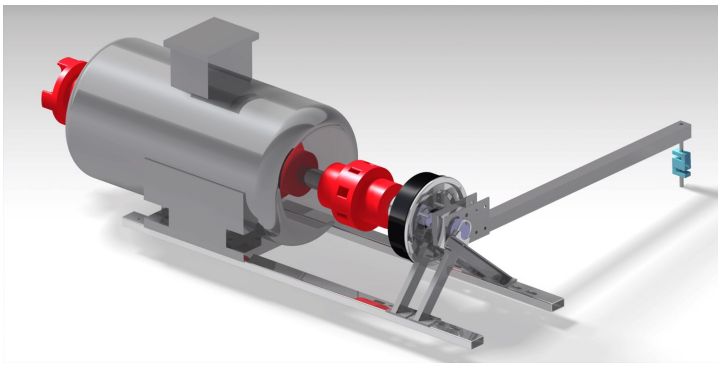

Figure 5.3: The setup as situated in EWI.

In the figure a simplified overview is given of the total system. The drum of the brake is connected to the axis of the DC motor via a coupling piece, which absorbs a significant part of the vibrations between the motor and the brake. The motor itself is connected to an inverter, which is able to let the motor spin at specific angular frequencies. The inner part of the brake is connected to the horizontal bar. The motor is only allowed to spin in the direction such that when the brake is activated, a force is measured that points downwards on the end of the bar. At that end a force sensor is located that measures the braking force. The inverter allows the axle to spin at fixed angular frequencies, which can be translated to velocity when the radius of the wheel of the trailer is known, using Equation 5.5.

$$v_{trailer} = \omega_{axle} \cdot r_{wheel} \tag{5.5}$$

By doing so, the influence of the speed to the braking force can be included. The braking force itself also needs to be converted to the braking force of the wheels. Equation 5.4 can be used for this purpose and by replacing the correct variables it becomes:

$$F_{wheel} = \frac{x_{sensor}}{x_{wheel}} \cdot F_{sensor} \tag{5.6}$$

where F_{wheel} is the braking force per wheel of the trailer and x_{cell} and x_{wheel} are the distances of the center of the axle to the force sensor and the axle to the ground, respectively.
The reason that this test set-up has been built, is to test the brakes in quarantine. The amount of side effects is limited that will occur during outdoor testing, such as loss of grip of the tires, or rain and dust that might interact with the stopping power. Also, the effect of rise in temperature can be perfectly determined and studied. Inside the brake thermocouples have been placed, which monitor the temperature at different crucial parts: the shell of the solenoid, the small braking shoe and two on the large braking shoe, one on each side. The large braking shoe has two thermal sensors, because it has a self-clamping side and a loose side. The self-clamping, better known as self-energizing effect occurs when the brake shoe gets dragged into the rotation of the drum. This increases the braking force without supplying extra energy to the drum brake. This side of the shoe will warm up more quickly because of the local increase in friction.
To simulate the wind that the brakes experience while driving, a centrifugal fan is added. When this will be left out, the brakes will heat up more quickly then they would when used on a trailer. The test set-up is used to eliminate certain side effects and unforeseen conditions, but still has to be as realistic as possible.

5.3.2. Car set-up

The second set-up that has been used is a trailer on which the electric brakes are mounted. A force sensor is also installed in the front of the trailer, which can measure the force between the car and the trailer. From within the car a DC source is connected to the solenoids inside the electric brakes, and the current can be tuned very precisely to achieve accurate braking forces. In this way, practical effects can be coped with and implemented in the LUT. The trailer is installed with Labview, a program that can read out the force sensor and thermocouples. This is a system that is proven to work and sends processed and filtered data to the computer. The installed system is solely for logging and collecting measurement data. The system does not control or influence the installed brakes.

5.4. Implementation

Both the EWI set-up as the car set-up have been tested and various results were obtained. First the results per set-up will be discussed, followed by the combination of results used for the LUT implementation.

5.4.1. EWI set-up

As mentioned before, at the EWI set-up, the inverter was able to let the axle turn at a constant angular frequency. Steps of 10 Hz were taken and the current was increased in steps of 0.5 A. The results can be seen in Figure 5.4.

The figure shows a rather chaotic plot. This is due to the amount of uncontrollable parameters during testing. For example, at consecutive runs the brake might heat up from the inside, but the heat at the outside is dissipated rather quickly. Since the temperature sensors are located on the outside of the braking pads, this cannot be measured. As a result, the brakes will heat up more quickly because of the higher temperature inside.
Another uncontrollable effect is due to that the brake cannot be activated instantaneously at the right current. During early testing the high peak forces caused by the abrupt clamping of the braking pads to the drum, completely bent the test setup, creating an unsafe situation. Therefore, after replacing the bent parts, the current is increased slowly by hand, thereby omitting the high peak forces. At high angular frequencies the braking force will increase approximately with the same speed, but the high speed of the drum creates more heat generation than the same braking force at lower angular frequencies. Again, the temperature will rise sharply compared to low angular rates, with more uncertain results as a consequence.

Despite the uncertainties, the results give a good impression of the capability of the brakes at certain currents. To give a first estimation of the performance at higher currents, the graph is extrapolated. For every frequency three extrapolation methods are considered: linear, cubic and spline. The method is chosen based on the expected characteristics of the brake. The expectation is that the braking force will increase with increasing currents, but also tends to saturate. The saturation is caused by the increase in temperature at higher braking forces. At high temperatures the generated friction will be lower due to fading [15].

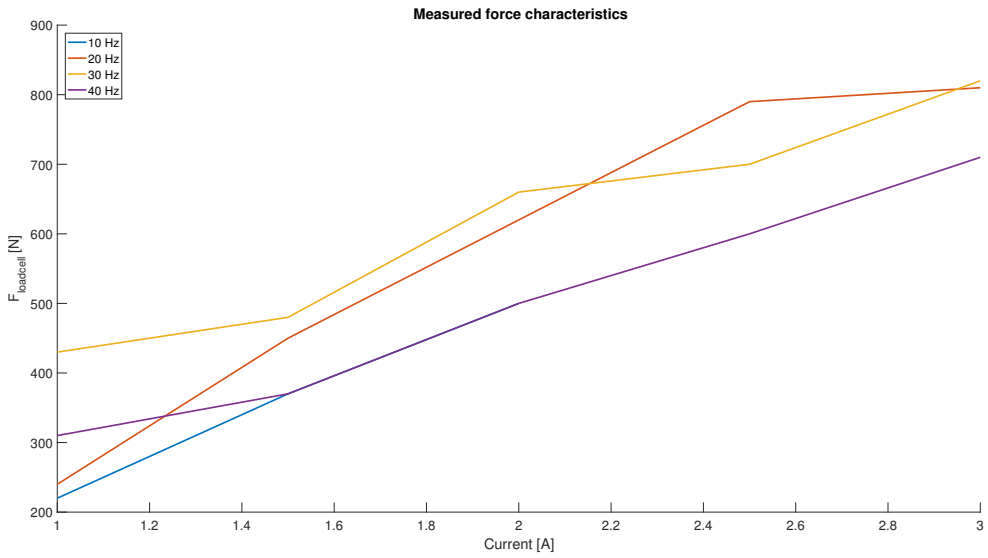

Figure 5.4: The results of the EWI set-up.

The resulting extrapolated graphs are shown in Figure 5.5.

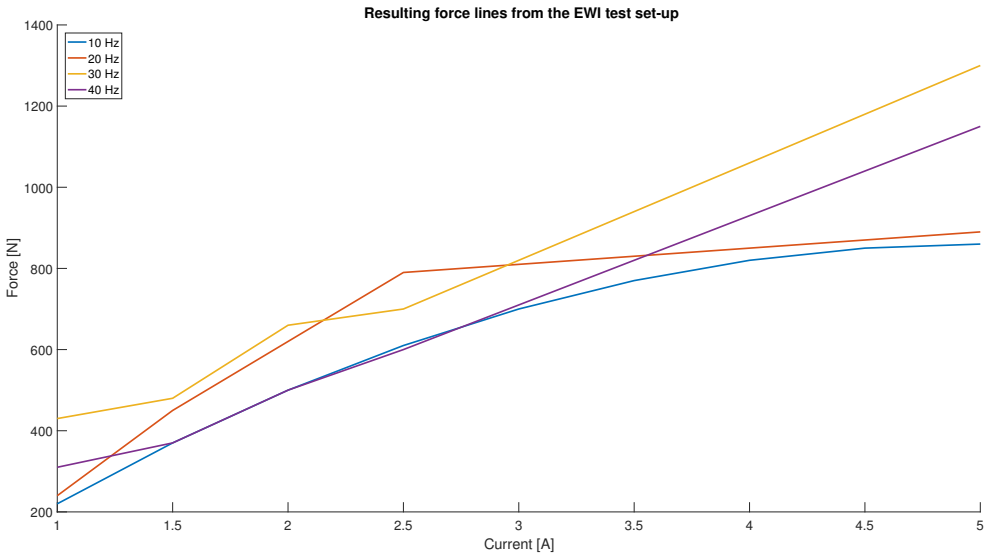

Figure 5.5: The extrapolated resulting plots to be verified.

In the above figure, extrapolation is used to determine the behavior at higher currents. The inverter could not deliver enough power to keep rotating when 3 A was flowing through the solenoid.
As can be seen, the results show a rather peculiar course of generated braking force. At low angular frequencies, the braking force is almost the same as at high rotational speeds. The 40 Hz (approximately 90 kph) measurement has the same behaviour in the low current region as the 10 Hz (approximately 20 kph) measurement. Another notable result is that the 20 Hz line tends to saturate, whereas the 30 Hz line is rising with increasing currents.

The exact behaviour of the brakes in the trailer should be checked for the different currents. Therefore, the test set-up available in the form of a car with a force sensor in the hitch connection is used.

5.4.2. Car set-up

The results from the car show a more linear behavior than the EWI set-up results, as depicted in Figure 5.6.

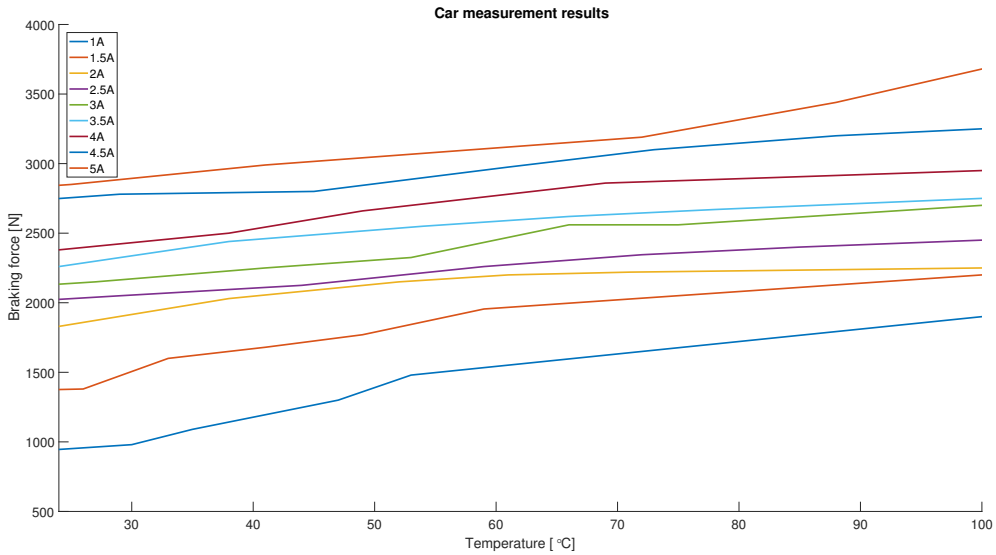

Figure 5.6: The results of the car tests.

Here it is clearly visible that an increase in current leads to an increase in braking force. Besides that, the braking force also increases as function of the temperature. The reason for this is that brakes have an optimum temperature. At this temperature the stopping power reaches a peak. For lower temperatures, the braking material is still very hard, but at higher temperatures the resin inside the brakes [2] starts to get more sticky, thereby increasing the coefficient of friction from Equation 5.3.

From the gathered data, a LUT is created, which combines the data of both the plots of Figure 5.5 and Figure 5.6. The LUT needs to be verified and adjusted during practical tests with the complete E-Brake system.

6

Results and verification

In this chapter the results of the subsystems of the BCU are presented, along with the results of the total E-Brake.

6.1. Overview

The subsystems of the BCU were tested during two testing days. At those days a car was used with a trailer mounted behind it. During several braking sessions the force sensor data was logged, together with the calculated braking force from the MPU, the calculated duty cycle from the current control, and the current that flows through the solenoid sent by the current control. The only subsection that was not tested is the power supply, which has been replaced by a DC/DC converter of Delta. The reason for this was that the designed DC/DC converter was not tested yet at the start of the testing days. For safety reasons the converter was left out and replaced by a converter that is tested thoroughly.

6.2. Testing and results

Instead of verifying the DC/DC converter during the testing days, the converter is simulated and fine tuned in LTspice, a simulation software of the manufacturer of the used LTC3787 chip. The results can be found in Figure 6.1. A zoomed version can be found in section A.1.

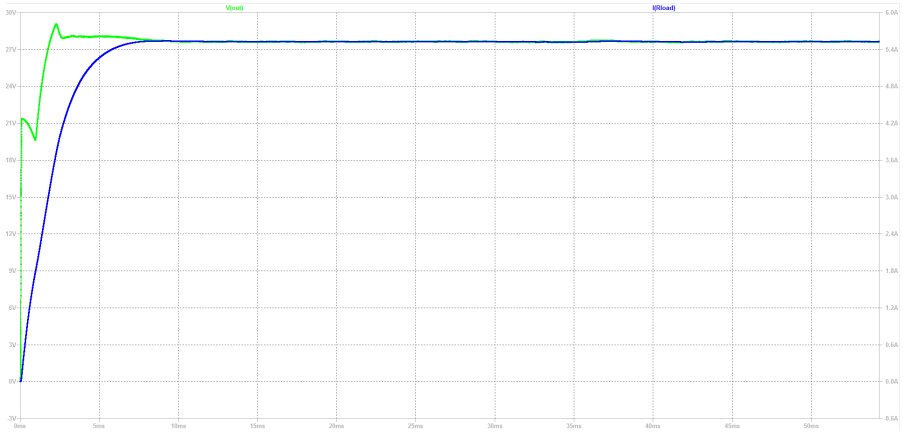

Figure 6.1: The simulation of the designed DC/DC converter.

The green line is the output voltage of the converter and the blue line is the output current.
For this simulation, a load resistance of 5 Ω was added to the output of the converter in series with an inductor

of 8 mH. This resistance was the actual resistance of the solenoids that were installed in the trailer at 60 °C. The input voltage was kept at 12 V, which is the rated battery voltage.
In the figure a small voltage overshoot of $\frac{29-28}{29} \approx 3.5\%$ is depicted, after which the converter settles at a stable 28 V and 5.6 A. The current increases more gradually, because the inductor has to store energy in its magnetic field.

The DC/DC converter should be able to work properly for input voltages between 11 and 13 V. These voltages correspond to an empty and a fully charged battery, respectively. In Figure 6.2a and Figure 6.2b the input source is set to 11 V and 13 V. The zoomed versions can be found in section A.2 and section A.3, respectively.

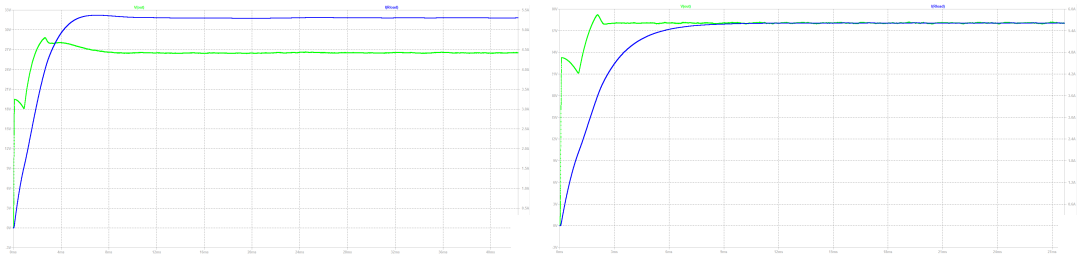

(a) V_{in} = 11 V. (b) V_{in} = 13 V.

Figure 6.2: The response of the DC/DC converter for the minimum and maximum value of V_{in}.

As can be seen, the converter works as designed. The overshoot is low and happens in a very short period of time. The time constant of the solenoid itself is 2.7 ms at 3 Ω, as stated in section 4.4. Because the simulation is done at 5 Ω, the expected time constant is $\frac{L}{R}$ = 1.6 ms. The time constant that is showed in the figure is approximately 2.14 ms. The reason that the time constant differs from the expected time constant, is that the input voltage is not a constant 28 V. In the calculation of $\frac{L}{R}$, it is assumed that the input voltage is constant, whereas in the simulation the converter has to start up. This leads to a lower initial voltage, resulting in a higher time constant.

The current and voltage ripple is obtained by zooming in to Figure 6.1, as shown in Figure 6.3.

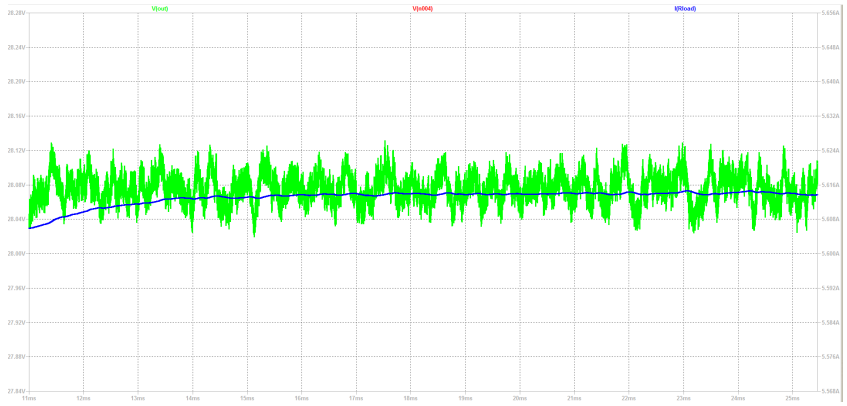

Figure 6.3: The current and voltage ripple at the output of the converter.

The figure shows that the voltage ripple is a maximum of 0.1 V, and the current ripple is a maximum of 0.02 A. At the worst case scenario, the voltage ripple induces a current ripple of 67 mA, which is tolerable for this purpose.

For the verification of the current drive module, practical measurements have been performed. The simulations that were done, describe the behaviour of the current through the coil depending on the duty cycle. The main requirements are that in the worst case, the ripple of the current in the coil remains below 50 mA and that the steady state current is the same as the aimed current. The simulation runs the worst case scenario of the system, which is represented by a current of 4.57 A, as derived in subsection 4.5.1. Figure 6.4 shows

a picture of a simulation done on the solenoid that is being charged with a PWM switching frequency of 20 kHz:

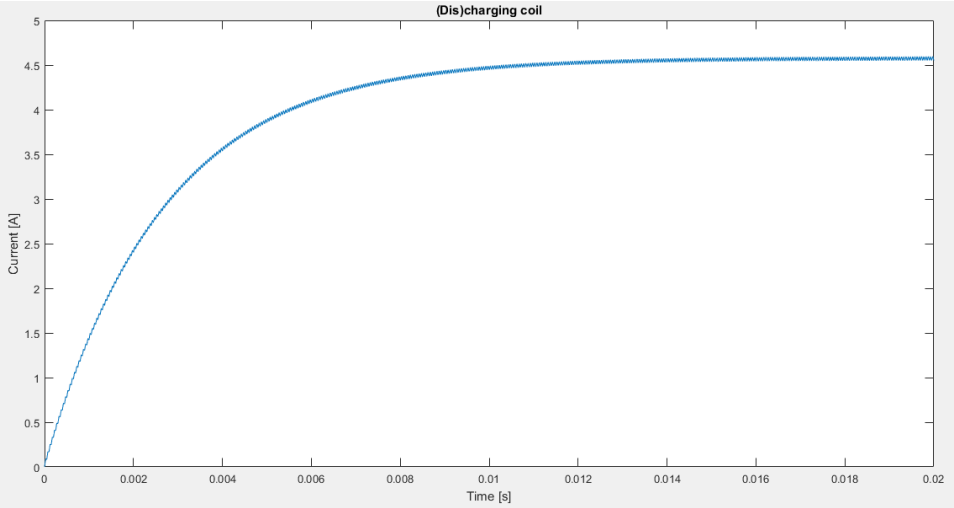

Figure 6.4: Charging the solenoid with a switching frequency of 20 kHz

Zooming in on the steady state switching region gives Figure 6.5:

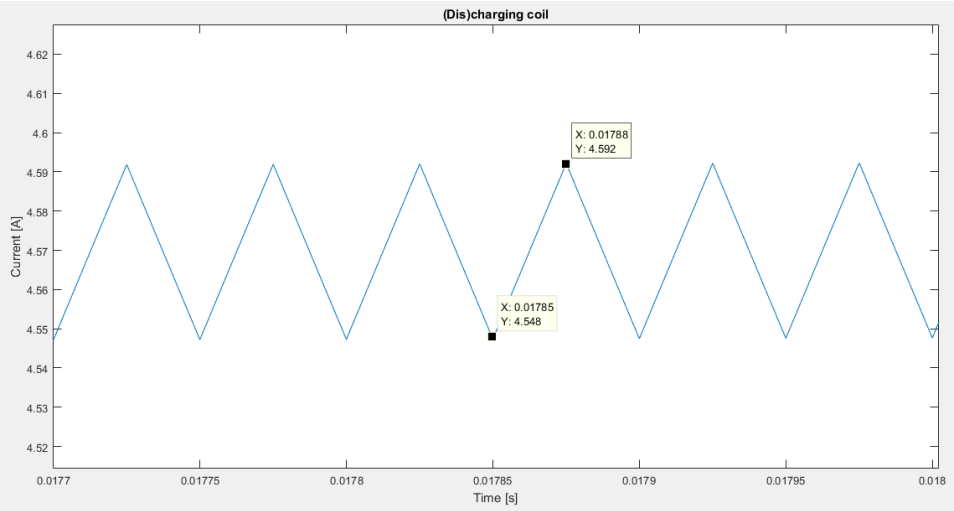

Figure 6.5: The current ripple at displayed at the switching frequency of 20 kHz

Furthermore, practical measurements have been performed to verify whether the right current was executed. For this, the limiter on the power supply was used. For different solenoids, the resistance had to be measured separately. The model was adjusted to the measured resistance. As a result, the calculated current deviation was below 100 mA which is sufficiently accurate. Because this was the case, the model was able to function properly as an open loop model for the testing days, since the current sensor did not work as expected.
The sensor was tested on the prototype separately from the other systems (MPU and HCU) and under constant currents. The assumption was made that it would work right in the whole system. However, the duty cycle and switching frequency caused the sensor measurements to deviate from the actual current. At a duty cycle of 0.2, the measured current was 3 times as high as the actual current. This deviation got smaller as the duty cycle increased more and more to one.

The last part that needs to be tested is the LUT. The LUT can only be tested in combination with the rest of the BCU, the MPU and the HCU. Therefore this part describes not only the verification of the LUT but also

the verification of all three systems combined.

The data that is presented at the output of the LUT should be verified by performing many braking sessions. During the sessions, the data from the force sensor is logged to check if the net force goes to zero. Besides the measured force, the calculated force from the MPU should also be logged. When the force sensor data goes to zero, the combination of the LUT and the controller of the MPU work properly.
First, a series of tests is done where the solenoids are decoupled from the power supply. The results can be seen in Figure 6.6.

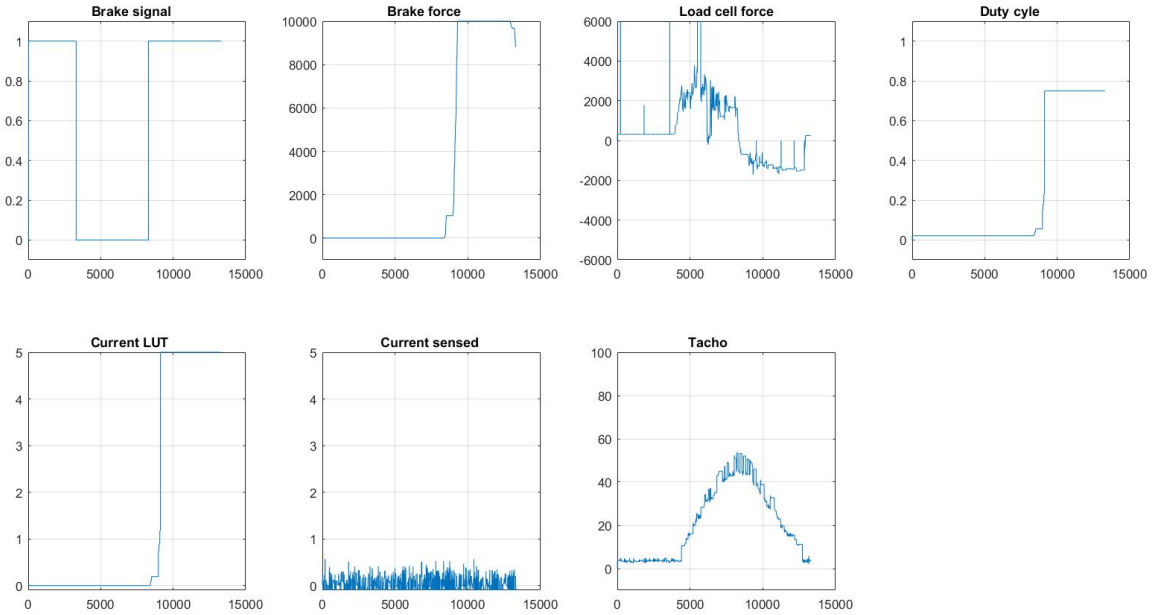

Figure 6.6: A braking session where the brakes are decoupled from the circuit.

In the figure several plots are shown, which are the logged data. The first plot is the braking signal of the car. When it is 0, the vehicle does not brake. When it is 1, the brake pedal is touched and the car brakes.

The plot on the right of it is the brake force, which is calculated by the MPU. A saturation limit was set in order to prevent that the controller kept integrating the braking force as it was not executed.

The load cell force displays the measured force between the car and the trailer by the force sensor. The area underneath the acceleration part (positive force) and the area underneath the deceleration part (negative force) are similar. This means that the total work is done by the car, both accelerating as well as decelerating.

For the duty cycle, a saturation limit was initiated as well. The used DC/DC converter from Delta was set at a maximum current, however the current had to be controlled by the PWM circuit. When the duty cycle would be set to 1, the maximum allowed current would have flown through the solenoids, with an emergency stop as a consequence. To safely test if the whole E-Brake system would work, the duty cycle was limited.

The current LUT plot shows the calculated output current for the received brake force of the MPU. The two figures look very similar, showing that the LUT is fast enough and proportional to the calculated current.

The current sensed diagram was used for the measurement of the output current that flows through the solenoid. During the testing days the signal was not logged properly and the sensor did not work as it was expected, as discussed in Figure 6.2.

Last, the tacho is the speedometer that was placed in the trailer as a verification of the driving speed. The speed of the car cannot be directly logged. For this reason a tacho meter was used.

To conclude, the figure shows that the brake force, current of the LUT and duty cycle all increase sharply. The saturation limits are met very quickly, indicating that the control loop integrates very quickly to reduce the error as fast as possible. This test also shows that the force sensor works properly, and the other systems react as expected.

A second test was a light braking test. After the car accelerated, the brake pedal was pushed lightly, initiating a slow stop. The goal was to see whether the system functioned as designed. The results are showed in Figure 6.7.

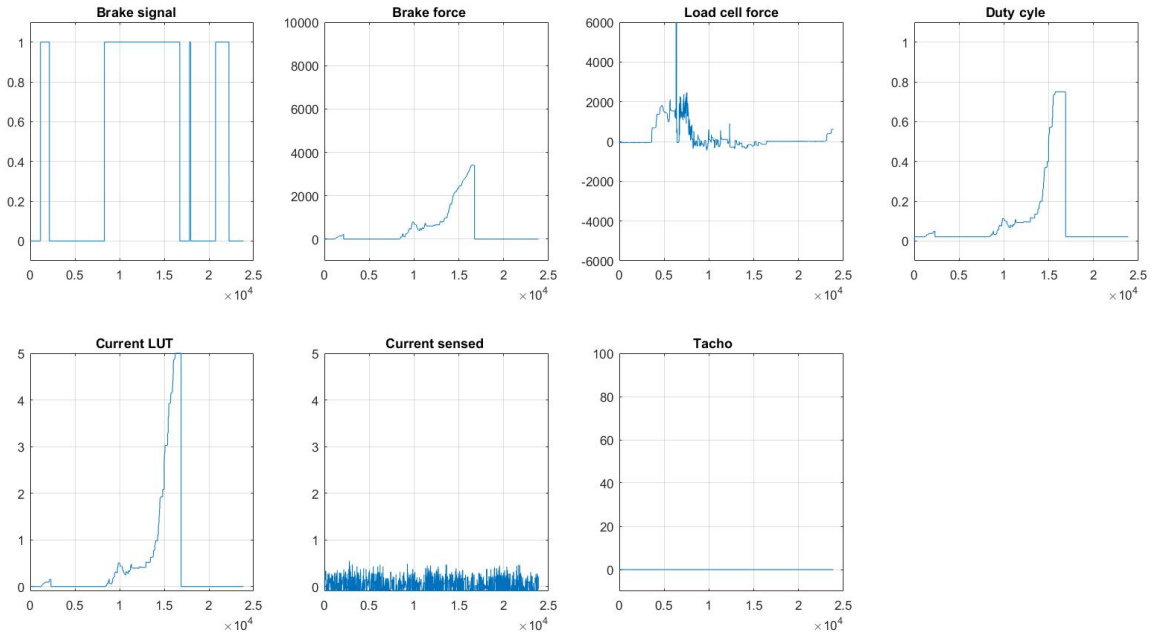

Figure 6.7: The braking session with the brakes activated. The brakes of the car brake lightly with increasing power.

In this test, the results are promising. The brake signal is activated from approximately $0.9{\cdot}10^4$ samples, and the car stands still at approximately $1.6{\cdot}10^4$ samples. In between this period, the car brakes with a small force. The brake force plot shows that the calculated braking power increases almost linearly. However, the load cell force plot shows that there is almost no force on the force sensor during the braking session. The duty cycle and current LUT plot show a linear increase as well, indicating that they follow up the calculated force.
The total result is that the trailer completely braked for itself during this test. The tachometer failed during the last tests because the batteries ran out of power. Therefore the data of the tacho meter is left out of this reflection. Figure 6.8 shows a close up of the most important signals, which are plotted in one figure.

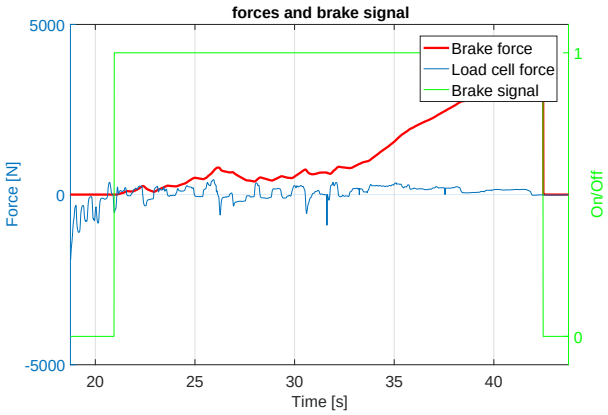

Figure 6.8: A close-up of the light braking session.

The plot zooms in on the moment where the brakes of the car are activated. As the braking force increases, the measured force remains balanced around zero. This indicates that the car brakes with an increasing force. Still, the complete system is able to regulate the braking force of the trailer such that it completely brakes for itself.

A third and final test is done, where the brakes are activated and an emergency brake is initiated. The expectation is that the measured force will not completely go to zero. However, the area under the deceleration curve should be smaller compared to the area underneath the acceleration plot. The test data is shown in Figure 6.9.

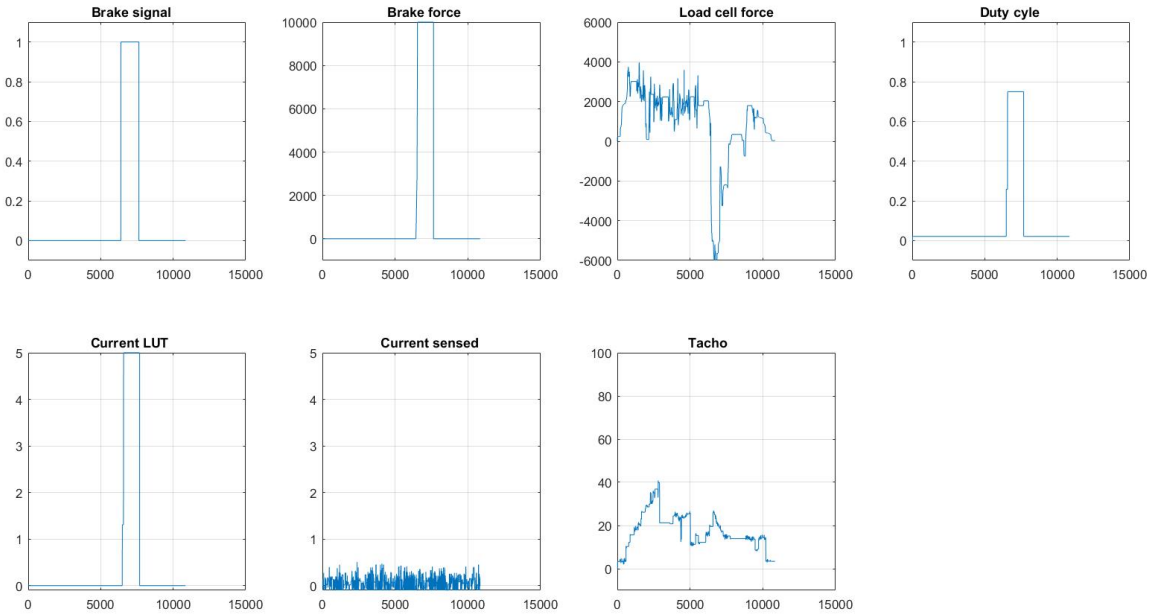

Figure 6.9: The braking session where the car makes an emergency stop.

As is shown in the figure, the force sensor immediately has a negative peak of 6000 N. This is the moment the car initiates its emergency stop. The control algorithm responds in the moments right after this, as can be seen in the load cell force plot. After the large peak, it decreases significantly. This is the moment that the limit of the current flows through the solenoids. The stopping power is not sufficient to completely eliminate the force on the car.

7

Discussion

The achieved results that were discussed in the previous chapter are not completely in line with the expectations. In this chapter the differences will be discussed.

The DC/DC converter was able to output a steady 28 V and 6 A. These specifications are derived from the characteristics of the solenoid. To make the converter more suitable for multiple sorts of solenoids, it should have a higher output voltage. Additionally, during extensive braking and wear to the solenoids, the internal resistance might increase with respect to time. The converter is designed such that it can meet the minimum voltage requirements. However, it would be better to create a margin on the voltage as well, just as with the current.

Besides the fact that the output voltage should be increased, the simulation results are as expected. The DC/DC converter meets the requirements, as can be seen from the figures in chapter 6. The plots show that the increase in current stagnates exponentially.
At the start-up, there is a small peak, after which the output voltage increases exponentially to the desired value. The exponential increase is caused by the SoftStart function of the converter. Instead of quickly and roughly achieving the output voltage, the start-up is regulated.

The model that was designed for the current also functioned as expected. The assumptions that the diode and the MOSFET could be modelled ideal and that the resistance of the current sensor could be neglected, turned out to be valid. The model actually was more accurate than expected.

The current controller that would regulate the current in case the model would fail, was not used during the testing days. This should be implemented for the case that the brakes get hotter and the resistance of the solenoids would increase. The calculation of duty cycle of the model would be wrong and consequentially the current would be wrong as well. For this reason, a better investigation on what current sensor is needed should be performed.

The ripple of the current in the solenoid was set to maximum 50 mA. The actual ripple was due to an extra applied margin, on the bottom boundary of the frequency. On top of the ripple, which turned out to be 44 mA, comes the ripple of the DC/DC converter which is 0.1 mV ripple. In the worst case scenario, the resistance of the coil is 3Ω. This voltage ripple causes an current ripple of 33 mA. The total current ripple becomes 77 mA. This still is not perceptible in the car, however was not taken into account beforehand.

As the tests have shown the LUT worked as designed. It follows the behaviour of the input force from the MPU. When the car braked softly, the complete control algorithm was able to reduce the force sensor data to zero. When the LUT would have outputted random values, the control algorithm would have clipped and overcompensate.

8

Conclusion

In this chapter, the complete design of the brake control unit will be discussed. The requirements that were applicable for the BCU are listed below for convenience.

1. The braking system should be able to regulate the braking action.
2. The maximum braking force has to be such that the trailer experiences a deceleration of at least 5.9 m/s^2.
3. The nominal maximum current consumption shall not exceed 15 A.

The derived requirements for each subsystem within the BCU were:

1. The power supply should be able to deliver at least 6 A at 27.6 V.
2. The power supply should be able to output 27.6 V for an input voltage range between 11 V and 13 V.
3. The current control should be able to regulate and the current flow through the solenoid.
4. The current control should accurately predict the flow of current, such that the open loop model represents reality sufficiently.
5. The LUT should be able to give a good estimation of the required current for a specific force.

As indicated before, the power supply meets all the stated requirements. The simulations indicated a stable circuit that is able to output 28 V and 6 A. The simulations also showed that the converter was able to output the required voltage when the battery was at its limits of 11 V and 13 V.
In addition to that, the converter showed a low voltage and current ripple, is affordable (total costs are under €50) and the LTC3787 chip is suited for multiple boost converters.

The current control model was successfully tested as an open loop model. It was able to predict and control the current through the solenoids by adjusting the duty cycle. This was done with a deviation lower than 100 mA and thus sufficiently accurate. As intended there was a closed loop model designed but due to complications with the current sensor this was not implemented.

After the complete design of the brake control unit, practical tests have been done to verify the working of the BCU within the complete E-Brake system.

9 Future work

With the end of the thesis, not all work is done yet. Several improvements can be made to the existing design and as sometimes opted in the text, some parts can be expanded.
In this chapter a view on future work is given. The work is meant to perfection the system as it is now. First, the DC/DC converter is discussed, followed by the current control and the LUT.

9.1. DC/DC converter

As mentioned in section 6.2, the DC/DC converter was not used during the testing because of safety reasons. The converter had to be redesigned several times and therefore was not tested thoroughly at the time of the testing days.
The first thing to do is to test the converter and use it in the car set-up. Caution should be paid regarding safety, as the converter handles power up to 224 W. Depending on the test results, a redesign should be made to optimize the behavior. Parameters that can be easily tuned are the switching frequency, the inductance of the coils and the output voltage.
One might want to increase the switching frequency when the output voltage ripple is too large. This will negatively influence the efficiency of the converter. There will always be a trade-off between ripple and efficiency.
When the inductor current will drop significantly during the OFF-state, the inductance needs to be increased. A larger inductor is able to store more energy in its magnetic field. As a consequence, it is able to deliver more power when during the OFF-state. The current drop will be reduced, such that constant current mode is guaranteed for the inductor.
Last, the output voltage can be adjusted by adjusting the feedback resistance of the DC/DC converter. When the observation is done that the voltage saturates, the feedback resistor should be reconsidered. When the resistance of the solenoid increases too much, the output current cannot be delivered.

9.2. Current control module

An issue that was noticed during heavy braking was that the MOSFETS get considerably hot. A small heatsink that was available was used as a cooling mechanism, however did not suffice.
Some good calculation on the heat production of the MOSFET should be done as this one does not suffice. The MOSFET needs to remain cool or else it is disadvantageous for its performance. If not watched closely it even could break down which is highly undesirable in a braking system that needs to be safe.

As discussed in chapter 7 the current sensor needs some further investigation in order to make it work properly.

During the testing days the resistance value of the solenoids in the model was adjusted to an all-round value.

This value was determined when the solenoids were at working temperature, around 60 °C. In order to make the model adjustable for every different solenoid under every temperature, its resistance should be measured. This can be done by using Equation 4.1, however since a current sensor already exists it is easier to implement a voltage sensor that measures the voltage across the solenoid.

9.3. Lookup Table

The values of the lookup table are based on new brakes. When using the brakes, the braking shoes will become thinner. The material will wear do to the continuous friction between the drum and the shoe. However, during all the tests, the braking shoes hardly erased.
When the brake has become thinner, the shoe has to travel a greater distance before reaching the drum. Consequently, the parameters of Equation 5.2 change with respect to time. The control loop of the MPU will have to correct heavily, when inaccuracies in the LUT occur during time.
A solution to this is to make the LUT self-adjusting. This can be implemented by making use of a script that checks the difference between the force that was asked for, and the force that was exerted. A threshold can be set when to replace a value in the table or create a new table with that value. When a set of braking shoes has completely worn out and is replaced, the LUT will be more accurate. The control algorithm does not have to correct a large error anymore, which improves the response time of the total system.

Bibliography

[1] Uniform provisions concerning the approval of vehicles of categories m, n and o with regard to braking. online, 3 2014. Regulations on Braking.

[2] Peter J Blau. Compositions, functions, and testing of friction brake materials and their additives. Technical report, Oak Ridge National Lab., TN (US), 2001.

[3] Roberto C Dante. *Handbook of Friction Materials and Their Applications*. Woodhead Publishing, 2015.

[4] H. El Fadil, F. Giri, O. El Magueri, and F.Z. Chaoui. Control of dc–dc power converters in the presence of coil magnetic saturation. *Control Engineering Practice*, 17(7):849 – 862, 2009. ISSN 0967-0661. doi: http://dx.doi.org/10.1016/j.conengprac.2009.02.004. URL `http://www.sciencedirect.com/science/article/pii/S096706610900032X`.

[5] Braham Ferreira and Wim Van der Merwe. *The Principles of Electronic and Electromechanic Power Conversion: A Systems Approach*. John Wiley & Sons, 2014.

[6] Brigitte Hauke. *Basic Calculation of a Boost Converter's Power Stage*. Texas Instruments Incorporated, 2009.

[7] C Hohmann, K Schiffner, K Oerter, and H Reese. Contact analysis for drum brakes and disk brakes using {ADINA}. *Computers & Structures*, 72(1–3):185 – 198, 1999. ISSN 0045-7949. doi: https://doi.org/10.1016/S0045-7949(99)00007-3. URL `http://www.sciencedirect.com/science/article/pii/S0045794999000073`.

[8] Gary L Johnson. Solid state tesla coil. *http://www. g3ynh.info/zdocs/refs/Tesla*, 2001.

[9] Marian K Kazimierczuk. *Pulse-width modulated DC-DC power converters*. John Wiley & Sons, 2015.

[10] S. Keeping. Understanding the advantages and disadvantages of linear regulators, 2012.

[11] Thomas A Lipo. *Introduction to AC machine design*. Wisconsin Power Electronics Research Center, University of Wisconsin, 2004.

[12] Robert Donald Lorenz and Lance P Haines. *Understanding Modern Power Conversion: Robert D. Lorenz and Lance P. Haines*. University of Wisconsin, 2000.

[13] Robert Donald Lorenz and Lance P Haines. *Understanding Modern Power Conversion: Robert D. Lorenz and Lance P. Haines*. University of Wisconsin, 2000.

[14] AL-KO International Pty Ltd. Comprehensive catalogue for vehicle technology, 2017.

[15] N/A. U.S. Army Materiel Command, N/A. ISBN N/A. URL `http://app.knovel.com/hotlink/toc/id:kpEDHADAB7/engineering-design-handbook-17/engineering-design-handbook-17`.

[16] The RV-Doctor. Electric trailer brake maintenance, 2002.

[17] Alexander Sadiku and Charles K Alexander. Fundamentals of electric circuits. *International Edition, Mc Graw Hill*, 2009.

[18] Zhanyou Sha, Xiaojun Wang, Yanpeng Wang, and Hongtao Ma. *Optimal design of switching power supply*. John Wiley & Sons, 2015.

[19] Linear Technology. *LTC3787 PolyPhase Synchronous Boost Controller*. Linear Technology Corporation, 2010.

[20] *Current Controlled Driver for 24-V DC Solenoid With Plunger Fault Detection.* Texas Instruments Incorporated, 2014.

[21] J. van Stappen. *Elektrisch Remmen.* E-Trailer, 2016.

[22] How A Car Works. Renewing drum-brake shoes, 2017.

[23] Henry J Zhang. Basic concepts of linear regulator and switching mode power supplies. *Linear Technology,[Online].Available:http://cds.linear.com/docs/en/application-note/AN140fa.pdf.[Accessed Jun. 2014]*, 2013.

A

Appendix

A.1. DC/DC converter simulation at V_{in} = 12 V

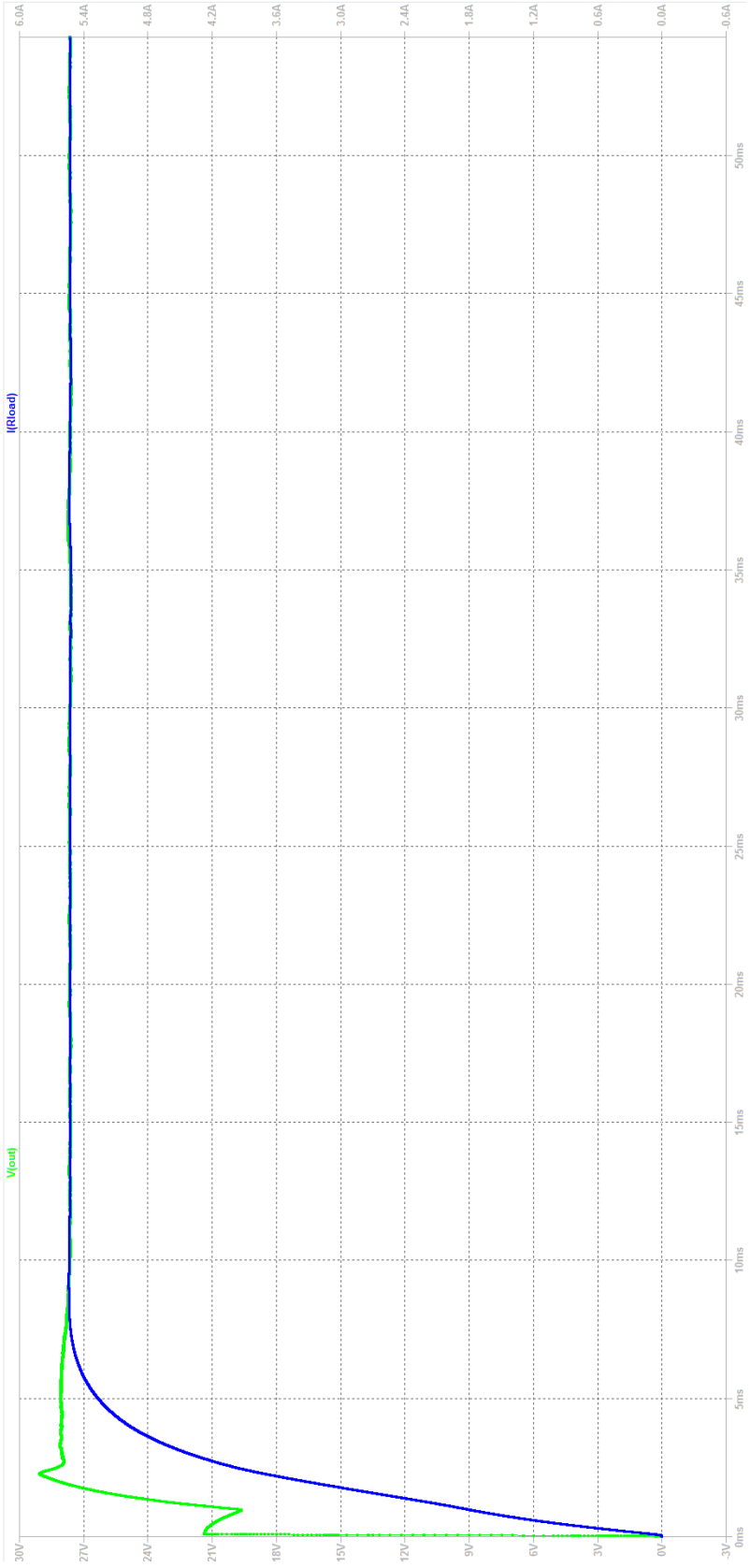

Figure A.1: The simulation of the designed DC/DC converter.

A.2. DC/DC converter simulation at V_{in} = 11 V

Figure A.2: The simulation of the designed DC/DC converter.

A.3. DC/DC converter simulation at V_{in} = 13 V

Figure A.3: The simulation of the designed DC/DC converter.